

WP 5 Projects

Title

Pilot & Demonstration projects

Projects (presented on the following pages)

Analysis of the Nowcasting System INCA-CH at Gletsch (VS)

Konrad Bogner, Matteo Buzzi, Massimiliano Zappa

In-situ stress and rock mass characterisation via mini-frac tests at the Bedretto Underground Laboratory

Kai Bröker, Xiaodong Ma and the Bedretto Lab Team

Heightening of very high gravity dams: the case study of the Grande Dixence

Basile Clerc, Giovanni De Cesare, Pedro Manso

Hydro-structural investigation of a 100 MW Francis turbine based on experimental tests and numerical simulations

J. Decaix, V. Hasmatuchi, M. Titzschkau, L. Rappilard, P. Manso, F. Avellan, C. Münch-Alligné

Control of sediment transport on an alpine catchment basin for the safe application of smart storage operations on an run-off-river HPP

Rafael Casimiro de Figueiredo, Jessica Zordan, Pedro Manso, Cécile Münch

Monitoring of small hydropower plants with a digital clone

Matthieu Dreyer, Christophe Nicolet, Anthony Gaspoz, Steve Crettenand, Cécile Münch Alligné

First insights on the production flexibility at the KWGO Power Plant

A. Gaspoz, V. Hasmatuchi, J. Decaix, C. Nicolet, M. Dreyer, J. Zordan, P. Manso, S. Crettenand, C. Münch-Alligné

HEATSTORE SWITZERLAND: New Opportunities for District Heating Network Sustainable Growth by High Temperature Aquifer Thermal Energy (HT-ATES) Storage

L. Guglielmetti, P. Alt-Epping, D. Birdsell, F. De Oliveira Filho, L. Diamond, T. Driesner, O. Eruteya, P. Hollmuller, M. Koumrouyan, Y. Makhoulfi, F. Martin, P. Meier, M. Meyer, J. Mindel, A. Moscariello, C. Nawratil de Bono, L. Quiquerez, M. Saar, R. Sohrabi, U. Spring, B. Valley, D. Van den Heuvel, C. Wanner

Atténuation dans l'espace cours d'eau des éclusées résiduelles d'un bassin de démodulation: cas d'étude de Piotta

Marie Loverius, Pedro Manso, Giovanni De Cesare, Samuel Vorlet

Directional-dependence of Mode I fracture toughness in Grimsel Granite

Morteza Nejati, Ali Aminzadeh, Martin Saar, Thomas Driesner

Computational Modelling of Fine Sediment Release Using SEDMIX Device with Thrusters

A. Onate-Paladines, A. Amini, G. De Cesare

Assessment of a turbine model to predict cost effectively the far wake of a hydrokinetic farm

O. Pacot, D. Pettinaroli, J. Decaix, C. Münch-Alligné

Large-scale Field Tests on Impuse Waves

Eva Sauter, Yuri Prohaska, Lukas Schmocker, Helge Fuchs, Robert Boes, Axel Volkwein

High Resolution Snow Melt and Runoff Modelling

Michael Schirmer, Massimiliano Zappa, Tobias Jonas

Multipurpose water reservoirs : a necessity for future irrigation?

J. Schmid, J. Decaix, C. Münch-Alligné, A. Gillioz

Set-up and configuration of an ensemble Kalman filter for an operational flood forecasting system

Anne Schwob, Alain Foehn, Javier Fluixa, Giovanni de Cesare

GPR imaging of fractures in the Bedretto Lab

Alexis Shakas, Peter-Lasse Giertzuch

Tracing the CO₂ pathway in a faulted caprock: the Mont Terri Experiment of the ELEGANCY-ACT project

Alba Zappone, Melchior Grab, Anne C. Obermann, Claudio Madonna, Christophe Nussbaum, Antonio P. Rinaldi, Clément Roques, Quinn C. Wenning, Stefan Wiemer

Analysis of the Nowcasting System INCA-CH at Gletsch (VS)

Konrad Bogner*, Matteo Buzzi** and Massimiliano Zappa*

*WSL, Zürcherstrasse 111, CH-8903 Birmensdorf; **Federal Office of Meteorology and Climatology MeteoSwiss

Motivation

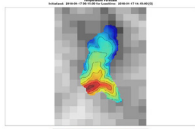
One objective of the **SmallFlex** project is to **increase the flexibility of the management** of the Small Hydropower Plant (SHP) by coupling the high resolution **now-cast system INCA-CH** and **COSMO-1** forecasts to predict the **inflow** for the next hours to days. This combined forecast system is implemented now at WSL and runs operationally since March 2018.

Study site



Gletsch catchment:
 Area: 39.8 km²
 Glaciation: 52%
 Mean elevation: 2719 m a.s.l.

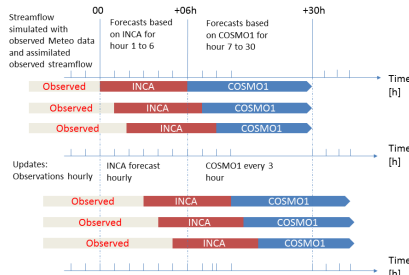
Example of INCA forecasts



1 km resolution of the INCA-CH model output (in grey) and the forecast downscaled to 100m by fitting Thin Plate Splines (TSP) to the surface taking the elevation as covariate.

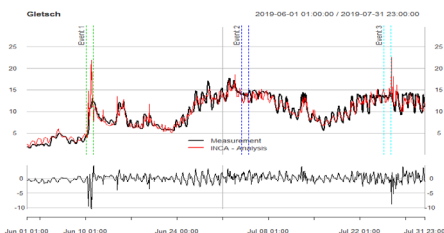
Operational forecast chain

Combination of the INCA-CH and the COSMO-1 based forecasts of the inflow having different initialization times and update intervals.



Data

The forecast system runs operationally since March 2018, but during the first year the runoff at Gletsch was mainly driven by glacier and snow melt processes. Thus, the analysis concentrates on June and July 2019, when two precipitation events have been predicted.



Series of the observed (black) and the analysis (lead time zero) of the INCA-CH predictions (red). The vertical lines indicate the three periods, which have been analysed in detail. At the bottom the error is shown.

Methods

Events driven by convective rainfall are highly localized and small deviations in the predicted direction and amount of the rain cells could lead to big errors. Therefore two machine learning (ML) based post-processing methods have been tested in order to reduce such error.

The methods used are¹:

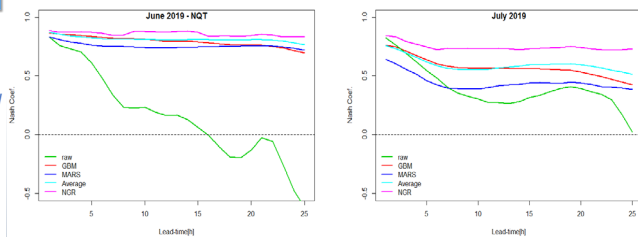
Gradient Boosting Method (GBM),

Multivariate Adaptive Regression Splines (MARS).

Additionally the different forecasts (raw, GBM, MARS) have been optimally combined by fitting a **Nonhomogeneous Gaussian Regression (NGR)**, which assigns more weight to the best performing forecast in the calibration period (i.e. previous 20 days).

Results

At first the Nash-Sutcliffe Efficiency has been estimated for June and July 2019 (see below). All post-processing methods show some significant improvements; the best results were achieved with NGR.

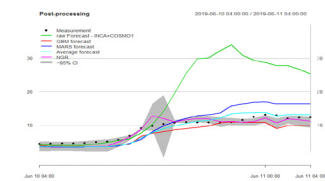


Nash Sutcliffe Coefficient for June and July 2019 for the raw and the post-processed forecasts

At next the three events are analysed in more details.

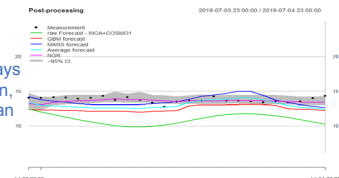
Event 1:

The timing of the beginning of the event is predicted very well, but the amount of rain was too high² resulting in overestimates of the runoff. Only after applying the post-processing the predicted inflow is within the range of the observed runoff.



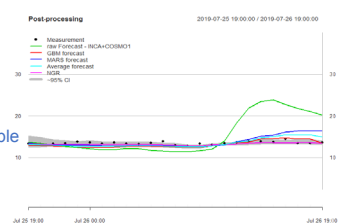
Event 2:

In order to test whether the post-processing is correcting the inflow always in the same direction a period is chosen, where the raw forecasts were lower than the observations.



Event 3:

This event is a false alarm, where the forecast showed quite a big event and nothing was happening in reality. The ML post-processor would have been able to identify this mistake and reduce the false peak accordingly.



Conclusions

The application of the INCA-CH system to such a small mountainous catchments reveals the sensibility of small shifts in the temporal and spatial evolution of thunder storms reflected by large errors. Thus it will be necessary to work with ensembles of such high resolution forecasts³ and to apply post-processing methods. First results of testing machine learning based error correction methods are shown highlighting the potential of such methods for improving the inflow forecasts.

References

- Bogner, K., Pappenberger, F. and Zappa, M.: Machine learning techniques for predicting the energy consumption/production and its uncertainties driven by meteorological observations and forecasts. *Sustainability*, 11(12), 2019.
- See also the Poster of Michael Schirmer, et al. for more details.
- Pulkkinen, S., Nerini, D., Pérez Hortal, A. A., Velasco-Forero, C., Seed, A., Germann, U., and Foresti, L.: Pysteps: an open-source Python library for probabilistic precipitation nowcasting (v1.0), *Geosci. Model Dev. Discuss.*, in review, 2019.

In-situ stress and rock mass characterisation via mini-frac tests at the Bedretto Underground Laboratory

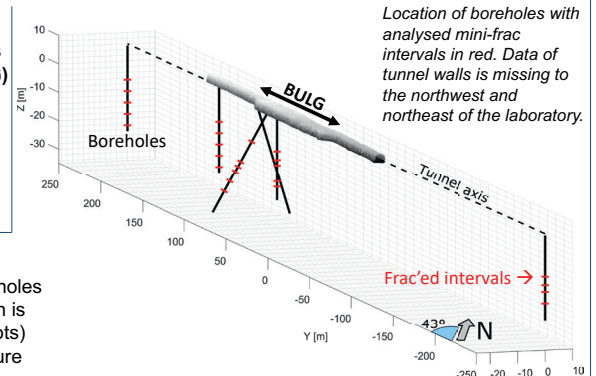
Kai Bröker^{1,2}, Xiaodong Ma^{1,2} and the Bedretto Lab Team

¹Swiss Competence Center for Energy Research – Supply of Electricity (SCCER-SoE)

²Geothermal Energy and Geofluids Group (GEG)

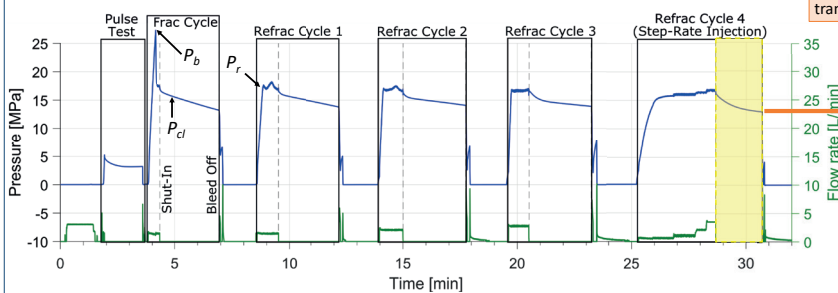
INTRODUCTION AND MOTIVATION

- Investigation of in-situ stress state (principal stress directions + magnitudes) and its variation around the **Bedretto Underground Laboratory for Geoenergies (BULG)** → located inside Bedretto tunnel, Canton Ticino
- Stress field determines hydraulic fracture initiation pressure + propagation direction
- Knowledge of stress state important for future creation of geothermal reservoir via **hydraulic stimulation**, especially for reactivation of pre-existing fractures linked to **induced seismicity**
- experiments carried out in crystalline rock (**Rotondo granite**), overburden ≥ 1 km

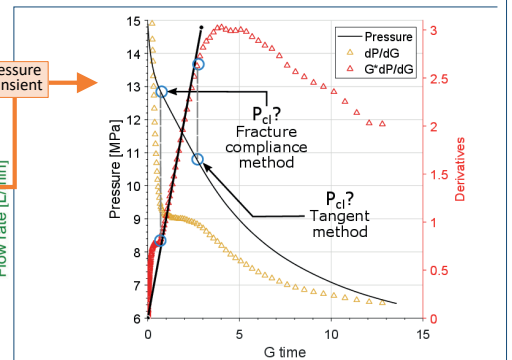


METHODS

- Mini-frac tests:** performed in four 30 m-long vertical + two 40 m-long inclined boreholes → estimation of formation breakdown (P_b) and fracture closure pressure (P_{cl}), which is \approx minimum horizontal stress (S_{hmin}), on different diagnostic plots (e.g. G-function plots)
- Extended shut-in times** (20 min, 1 hr, to 12 -14 hr): estimation of local pore pressure (P_p), when pressure derivative approaches zero
- Dry packer reopening test:** calculation of rock mass stiffness and evaluation of fracture reopening pressure (P_r) without interfering fluid flow effects due to residual aperture of fracture



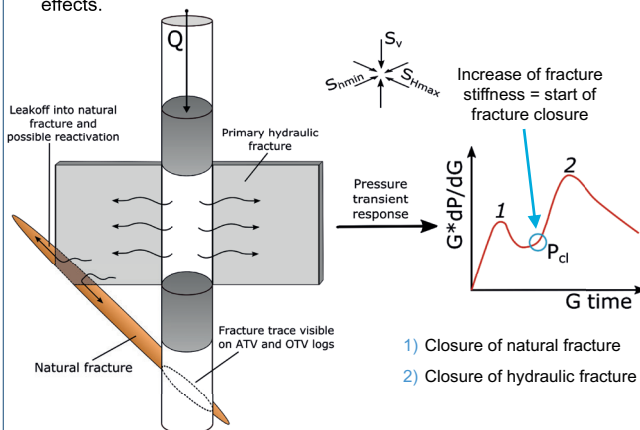
Injection protocol of a mini-frac test. Flow rate shown in green and interval pressure in blue. P_b is obtained from the initial frac cycle, P_{cl} from the transient after pump shut-in of every cycle and P_r from the refract cycles.



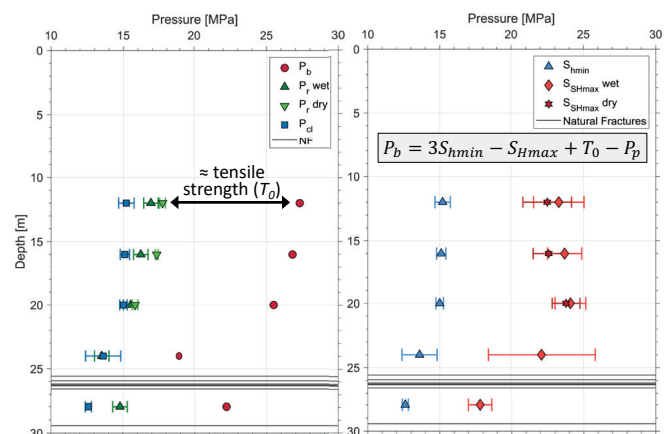
Data analysis example with pressure transient, its derivative and Bourdet derivative on a G-function plot to estimate fracture closure pressure according to two common picking methods.

RESULTS

- Fracture compliance method** by McClure *et al.* (2014, 2016) is applicable to crystalline rock mass to pick P_{cl} as estimate for S_{hmin} .
- G-function plots show comparable pressure transients between intervals, often two peaks visible in Bourdet derivative.
- Intra- and inter-borehole variations** of pressure values and stress magnitudes are identified.
- Proximity to **natural fractured zones** (identified using borehole logs) influences stress state.
- Dry reopening tests give higher P_r values than mini-frac tests.
- P_b between 2.4 – 5.3 MPa (below hydrostatic) indicates tunnel drainage effects.



Hydraulic fracture is likely to intersect natural fractures. Slip tendency analysis showed that pressure increase is sufficient for reactivation. → creation of **complex fracture network**



Results of vertical borehole SB3.1. Estimation of maximum horizontal stress (S_{hmax}) is based on the formula by Hubbert and Willis (1957). Variations of the stress magnitudes are visible on tenth of meters scale and the fractured zone around 26 m seems to decrease the stress magnitudes.

OUTLOOK

- Calculate matrix permeability from overnight shut-in pressure transients
- Estimate stiffness from wet- and dry- packer reopening tests → calibration of equipment needed
- Analyze remaining boreholes and intervals to characterize larger scale spatial variations (stress heterogeneity)

References

- M. Hubbert and D. Willis. Mechanics of hydraulic fracturing. Petroleum Transactions, AIME, 210:153-168, 1957.
M. McClure, C. A. Blyton, H. Jung, and M. M. Sharma. The effect of changing fracture compliance on pressure transient behavior during diagnostic fracture injection tests. In SPE Annual Technical Conference and Exhibition. Society of Petroleum Engineers, 2014. doi: 10.2118/170956-MS.
M. McClure, H. Jung, D. D. Cramer, and M. Sharma. The fracture-compliance method for picking closure pressure from diagnostic fracture-injection tests. SPE Journal, 21(4):1321-1339, 2016. doi: 10.2118/179725-PA.

Heightening of very high gravity dams: the case study of the Grande Dixence

Basile Clerc, Dr. Giovanni De Cesare, Dr. Pedro Manso

E-Mail: basile.clerc17@gmail.com; giovanni.decesare@epfl.ch; pedro.manso@epfl.ch

EPFL

Motivation

Dam heightening can provide large incremental positive impacts on storage with minimum incremental negative impacts, but requires deep knowledge of the structure and its foundation. Very high gravity dams are usually well studied and documented due to their importance and complexity. Such profound knowledge of the dam-reservoir-foundation system considerably reduces the uncertainty about site conditions already at an early stage of design. Furthermore, the availability of monitoring data and safety assessment tools (FE models, predictive behaviour models) strongly reduce the preparation time to reach feasible design solutions.

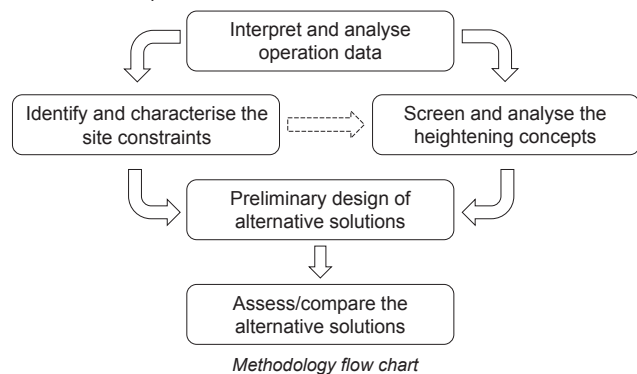
The Grande Dixence dam, located in the Canton of Valais, creates the largest reservoir in Switzerland, providing 10% of the country's storage energy. If heighten this dam could be used to transfer a larger share of the summer inflows to produce electricity in winter.



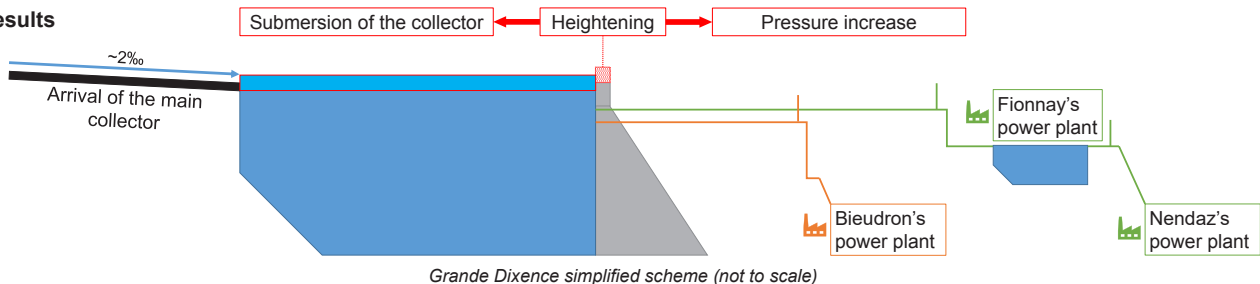
Top view of the Grande Dixence dam

Methods

The methodology consists of two main steps. The first step evaluates the reference state of the studied hydroelectric scheme to identify major constraints, while the second step consists of analysing and generating heightening solutions. The analysis of the results obtained during both prior stages should allow an assessment of the developed variants to determine the optimal solution.



Results



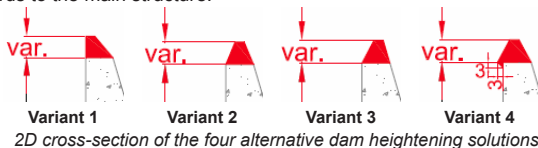
Screening of heightening concepts

Several heightening solutions were considered, but constraints were quickly acknowledged [1]. The plan shape of the dam crest strongly limits the integration of an arch and the presence of joints every 16 m is a strong constraint to any solution of buttress or multiple-arch heightening concepts.

Considering building artificial abutments and/or using post-stressed anchors was also investigated. However, the use of 300 m long anchors is technically unheard of and challenging and has been discarded.

In summary, due to its easier implementation and higher flexibility in regards to the geometry of the actual dam, a similar structural concept was preferred from inception when considering joint behaviour of the original and heightened structures.

This concept lead to retaining four alternative solutions for comparison, all with a new crest width of 5 m. Investigations cover height increase solutions from few meters up to maximum 30 m (~10% of the existing dam height). Key differences are the water column over the upstream face of the height increase and the location of its gravity centre with regards to the main structure.



Verification results analysis

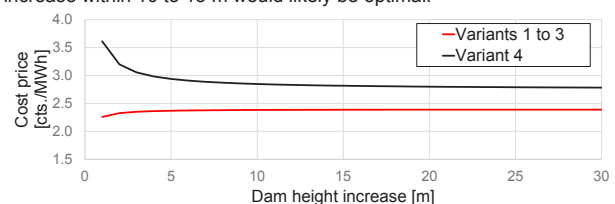
The verification analysis shows satisfactory results as all variants meet the design criteria.

Major constraints

As seen on the simplified diagram above, the height increase solutions would submerge the main conveyance tunnel outlet and the backwater effects modify pumping and aeration conditions farther upstream. Moreover, the water pressure increases on the waterways leading to both powerplants downstream: although Bieudron's surge tank can withstand the increase, Fionnay's cannot without adaptation measures.

Economic analysis

A preliminary analysis of the Levelized Cost of Electricity (LCOE) indicates a remarkably low cost price and point out that a height increase within 10 to 15 m would likely be optimal.



LCOE of the retained alternative concepts as a function of dam height increase

References

- [1] Clerc, B., Manso, P., De Cesare, G. (2019) Heightening of very high gravity dams: the case study of the Grande Dixence. International Benchmark Workshop on Numerical Analysis in Dams, Open Theme, Milan (in press).
- [2] Office fédéral de l'énergie OFEN. (2015). Directive sur la sécurité des ouvrages d'accumulation, Parties A à E.
- [3] Schleiss, A. J., Pougatsch, H. (2011). Traité de Génie Civil volume 17 : Les barrages. Presses polytechniques et universitaires romandes, Lausanne.
- [4] Schaeffli, B., Manso, P., Fisher, M., Huss, M., & Farinotti, D. (2019). The role of glacier retreat for Swiss hydropower production. Renewable Energy, Volume 132.

Hydro-structural investigation of a 100 MW Francis turbine based on experimental tests and numerical simulations

J. Decaix¹, V. Hasmatuchi², M. Titzschkau³, L. Rappillard², P. Manso⁴, F. Avellan⁵, C. Münch-Alligné²

¹ Institute of Sustainable Energy / ² Institute of Systems Engineering, School of Engineering, HES-SO Valais-Wallis, Rawil 47, Sion, Switzerland

³ Kraftwerke Oberhasli AG, Grimsel Hydro, Innerkirchen, Switzerland

⁴ PL-LCH / ⁵ LMH, EPFL, Lausanne, Switzerland

Motivation

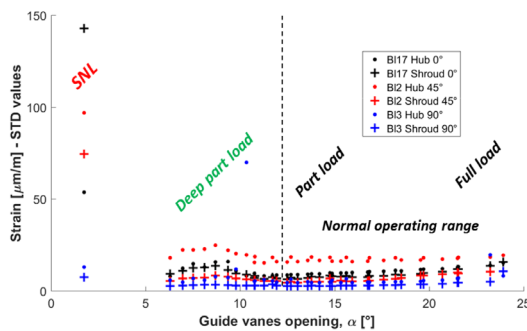
- ❑ Pumped-storage power plants: key components in a successful integration of renewable energies
- ❑ Hydraulic turbines and pump-turbines:
 - Operation in a wide range to offer power regulation flexibility;
 - Undergo frequent start-up and/or stand-by operating regimes;
 - Facing to harsh structural loadings with impact on their lifetime.

Objectives

- ❑ Achievement of a hydrodynamic instability level hill-chart of the machine;
- ❑ Investigation of the harmful conditions using experimental and numerical resources;
- ❑ Proposal of an alternative less-harmful start-up path and stand-by position with direct effect on the long-term maintenance costs;
- ❑ Elaboration of a diagnosis protocol to redraw hydrodynamic instability level hill-charts on different hydropower units using only a simplified instrumentation set.

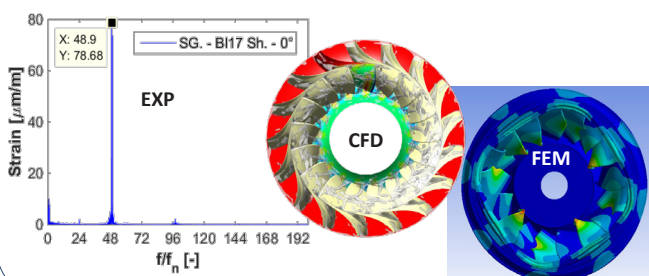
Hydrodynamic instability hill-chart

- ❑ Puts in evidence the high level of strain fluctuations observed on the runner blades at the Speed No-Load (SNL) operating condition characterized by a small opening angle of the guide vanes.



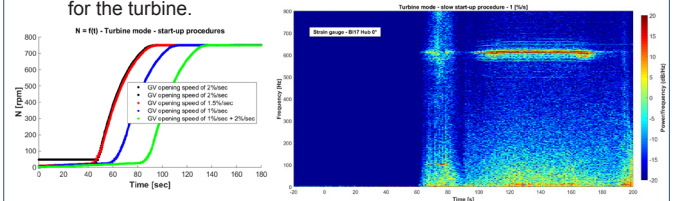
Investigation of harmful conditions

- ❑ Combining the experimental data with CFD and FEM simulations as well as the theoretical works, an origin for the high level of strain fluctuations has been proposed:
 - At the SNL operating condition, an Eigen mode of the runner is excited by an external source;
 - After several years of operation, the fatigue limit of the material is reached and cracks are observed at the trailing edge of the runner close to the hub.



Alternative start-up path

- ❑ Three alternative slower start-up procedures have been tested:
 - No beneficial effect noticed since the synchronization process remains unchanged.
- ❑ Synchronization procedure with the pump filled seems to be safe for the turbine.



Diagnosis protocol with a simplified instrumentation set



Main achievements



References

- [1] J. Decaix, V. Hasmatuchi, M. Titzschkau, L. Rappillard, P. Manso, F. Avellan & C. Münch-Alligné, 2019, "Experimental and numerical investigations of a high-head pumped-storage power plant at speed no-load", IOP Conf. Ser. Earth Environ. Sci., 240(8).
- [2] M. Titzschkau, V. Hasmatuchi, J. Decaix & C. Münch-Alligné, 2018, "On-board measurements at a 100MW high-head Francis turbine", Vienna Hydro 2018, Vienna, Austria.
- [3] V. Hasmatuchi, J. Decaix, M. Titzschkau & C. Münch-Alligné, 2018, "A challenging puzzle to extend the runner lifetime of a 100 MW Francis turbine", Hydro 2018, Gdansk, Poland.

Acknowledgements

Supported by:
 Schweizerische Eidgenossenschaft
Confédération suisse
Confederazione Svizzera
Confederaziun svizra
Swiss Confederation
Innosuisse – Swiss Innovation Agency

FlexSTOR

Partners of the FLEXSTOR - WP6 project (17902.3 PFEN-IW-FLEXSTOR)

Hes-SO VALAIS WALLIS
School of Engineering

EPFL
ÉCOLE POLYTECHNIQUE
FÉDÉRALE DE LAUSANNE

YKWO
GRIMSELSTROM

Control of sediment transport on an alpine catchment basin for the safe application of smart storage operations on an run-off-river HPP

Rafael Casimiro de Figueiredo; Jessica Zordan*; Pedro Manso, Cécile Münch
Plateforme en Constructions Hydrauliques (PL-LCH), École Polytechnique Fédérale de Lausanne (EPFL)*Corresponding author: jessica.zordan@epfl.ch

EPFL

Objectives

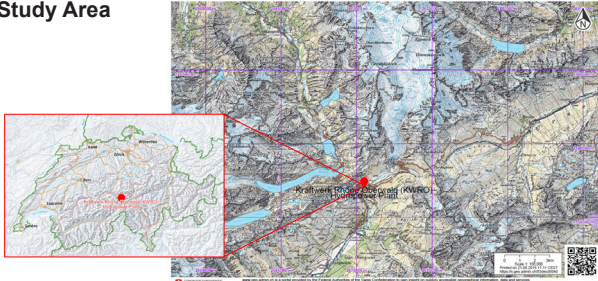
Smart storage operations (SSO) have been implemented on an alpine run-off-river HPP (case study: KW Gletsch-Oberwald HPP) in order to enhance the flexibility of the power plant (ref poster SmallFlex). SSO operations consist on the use of available space underground, such as the settling basin, in order to store the water, particularly in periods of the year with low inflow, which can afterward be used for energy production when the demand and the remuneration tariffs are higher and at a discharge close to the optimum of the turbine to have the best efficiencies¹.

The aim of efficiently implementing the SSO operations on the settling basin requires sediment management in order to assure a safe use of this part of the system whose function is temporarily changed. In order to understand the amount of sediment inflow into the settling basin, the following actions were undertaken:

- Determine the amount of potential mobilized sediments at the catchment scale with the use of Beyer-Portner (1998) and Gavrilović (1990) formulas;
- Determine the maximum sediment transport capacity of the river Rhone upstream the intake with the use of Beyer-Portner (1998) formula.

This will allow to verify in which periods of the year the sediment basin can be used for water storage with no risk related with sediment conveyance into the waterways and therefore at the turbines.

Study Area



Gletsch catchment⁶

- Surface area: 40.34 km²
- Average altitude: 2691m a.s.l.
- River principal watercourse length: 3450m
- River secondary watercourse length: 3870m
- River discharge: 2.93m³/s
- Average slope along the course: 13.7%

Procedure

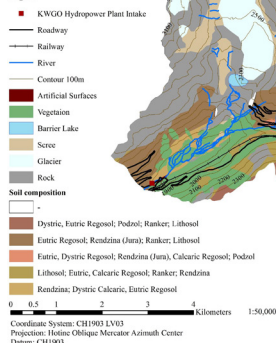
Soil coverage analysis

The map was created to display the land use of the case study. The values produced for calculating the erosion models and sediment transport model.

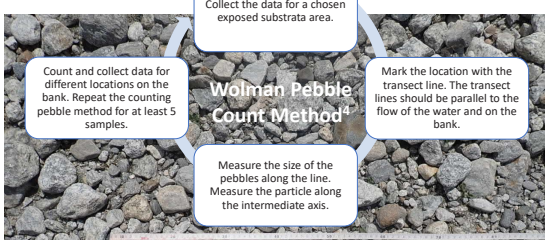
Land use⁶:

- Vegetation: 5.1 km²
- Open spaces with little or no vegetation: 15.9 km²
- Lakes and rivers: 0.2 km²
- Glaciers and perpetual snow: 18.8 km²
- Artificial surfaces: 0.3 km²
- Erodible soils: 15.5 km²

Legend



Pebble count

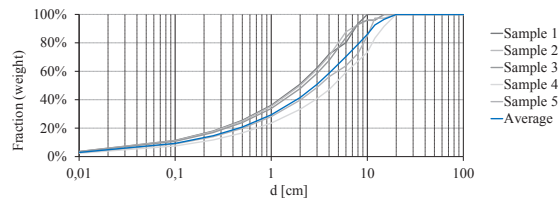


Results

Grain size distribution

The analysis of the measurements following the Pebble count method resulted in the compilation of the following grain size distribution:

$d_{90} = 5.8\text{cm}$, $d_{84} = 3.8\text{cm}$, $d_{65} = 4.2\text{cm}$, $d_{50} = 3.6\text{cm}$ and $d_{30} = 1.0\text{cm}$.



Erosion Model Calculations

Beyer-Portner formula²

$$V_A = 93 \cdot 10^{-15} \cdot H_{\text{été}}^{0.052} \cdot SE^{0.091} \cdot SV^{8.108} \cdot \Delta L_G^{0.082} + 274$$

$$V_A = 93 \cdot 10^{-15} \cdot 323.8^{0.052} \cdot 38.54^{0.091} \cdot 39.38^{8.108} \cdot 0.44^{0.082} + 274$$

$$V_A = 275.41 \text{ m}^3 \text{ km}^{-2} \text{ an}^{-1}$$

$$V_A = 11110 \text{ m}^3/\text{year}$$

V_A	Specific volume of annual sediment input [m ³ km ⁻² an ⁻¹]
$H_{\text{été}}$	Average rainfall between June and September [mm]
SE	Percentage of the catchment area made up of erodible soils [%]
SV	Percentage of watershed area without vegetative cover [%]
ΔL_G	Annual change in glacier length relative to total length [%]

Gavrilović method³

$$W_a = T \times P_a \times \pi \times \sqrt{Z^3} \times A$$

$$W_a = 0.8 \times 323.8 \times \pi \times \sqrt{0.5^3} \times 40.3$$

$$W_a = 11915.4 \text{ m}^3/\text{year}$$

W_a	Total annual volume of detached soil [m ³ /year]
T	Temperature coefficient
P_a	Average annual precipitation [mm]
Z	Erosion coefficient
F	Study area [km ²]

Sediment Transport Model Calculations

Smart and Jaeggi formula⁵

$$q_B = \frac{4}{(s-1)} \cdot \left(\frac{d_{90}}{d_{30}}\right)^{0.2} \cdot q \cdot J^{1.6} \cdot \left(1 - \frac{\theta_{cr}(s-1)d_{90}}{h_m \cdot J}\right)$$

$$q_B = \frac{4}{(2.65-1)} \cdot \left(\frac{0.058}{0.010}\right)^{0.2} \cdot 0.74 \cdot 0.14^{1.6} \cdot \left(1 - \frac{0.05(2.65-1) \cdot 0.036}{0.2 \cdot 0.14}\right)$$

$$q_B = k \cdot q = 0.13 \cdot q \text{ m}^3/\text{s m}$$

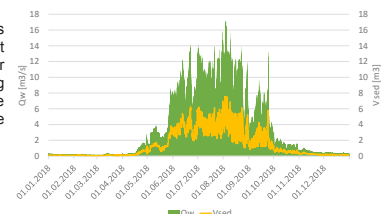
q_B	Specific sediment discharge (net sediment volume per time per unit width) [m ³ /s m]
$s = \frac{\rho_s}{\rho}$	Relative density of sediment to water [-]
d_{30}, d_{90}	Characteristic grain sizes, 30% or 90% (by weight) of the bed material are smaller [m]
d_{50}	Mean grain size [m]
q	Specific water discharge per unit width [m ³ /s m]
J	Slope
θ_{cr}	Critical Shields factor at beginning of motion
h_m	Mixture (water and sediment) flow depth [m]
K	Sediment transport model linearization between specific water and sediment discharges

Discussion

A detailed analysis of the catchment characteristics, in terms of **soil coverage** and **grain size**, has allowed to investigate the potential sediment input to the KWRO hydropower plant. It has been found that the sediments volume available at the catchment scale is limiting the effective sediment inflow i.e. the sediments transport capacity is reduced by the sediments availability.

The sediment transport formula has been used to calculate the sediment discharge as a function of the water discharge and linearly distributing estimated sediment availability. The hourly sediment volume at the intake can therefore be calculated as:

$$V_{sed}(h) = \frac{k Q_w(h)}{(325 \times 24)/W_a}$$



References

- First insights on the production flexibility at the KWRO Power Plant, Smallflex Project, SCCER-SoE Annual Conference 2019
- Beyer Portner, N. (1998). *Communication: Erosion des bassins versants alpins par ruissellement de surface*. Lausanne: Communications de Laboratoire de constructions hydrauliques, Ecole Polytechnique Fédérale de Lausanne.
- Dragičević, N., Karleuša, B., & Ozanic, N. (2017). *Erosion Potential Method (Gavrilović Method) Sensitivity Analysis*. Rijeka: Soil.
- Harrison, C., Rawlins, C., & Potyondy, J. (1994). *Bed and Bank Material Characterization: An Illustrated Guide to Field Technique*. Colorado: United States Department of Agriculture.
- Smart, G., & Jaeggi, M. (1983). *Sediment Transport on Steep Slopes*. Zürich: Mitteilungen der Versuchsanstalt für Wasserbau, Hydrologie und Glaziologie.
- Swiss Confederation. (2019, July 15). *Maps of Switzerland*. Retrieved from map.geo.admin.ch: <https://map.geo.admin.ch/>

Monitoring of small hydropower plants with a digital clone

Matthieu Dreyer, Christophe Nicolet, Anthony Gaspoz, Steve Crettenand, Cécile Münch-Alligné

SmallFlex motivation

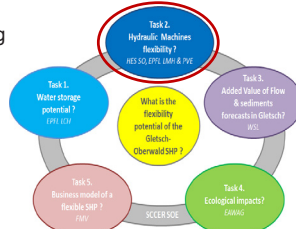
- To show how small-hydropower plants (SHP) can provide winter peak energy and ancillary services, whilst remaining eco-compatible.

Overarching research question

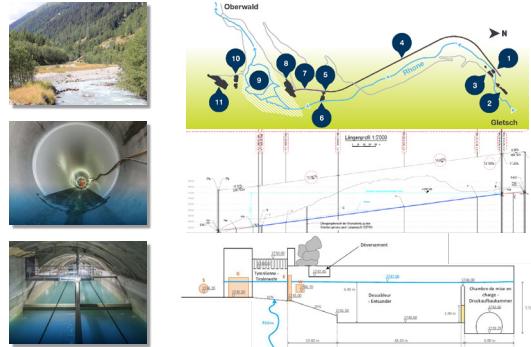
- What are the consequences of enlarging the operational range of the Pelton turbines in case of large head variations?

Hydro-Clone® contributions

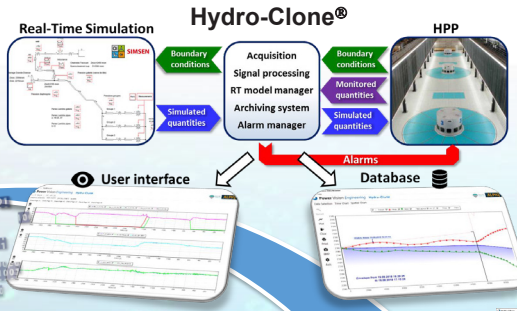
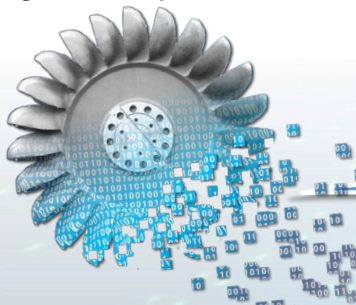
- Monitoring of the power plant
- Estimation of the available power/energy for ancillary services



Demonstrator site : the Glatsch-Oberwald SHP



Digital clone implementation



Live monitoring and data archiving

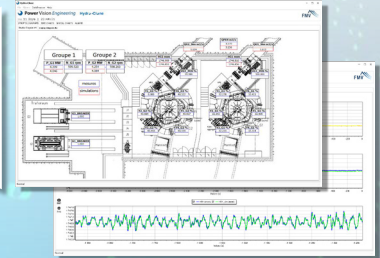
- Monitoring of non-measurable quantities
- Detection of abnormal pressure transients prior to reach admissible limit
- Detection of Hydraulic/Electrical anomalies
- Anticipation of power plant damages

Numerical modeling of the power plant

- Complete 1D-model of the power plant with SIMSEN
- Calibration of the model based on powerplant real operating sequences

Hydro-Clone real-time simulation

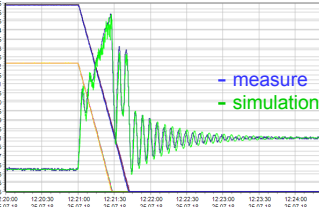
- Real-Time numerical "cloning" using the complete 1D-model of the power plant
- Boundary conditions measured in-situ and fed to the model in real-time
- Data processing and diagnosis of the power plant health



Benefits and outcomes from real-time simulation monitoring

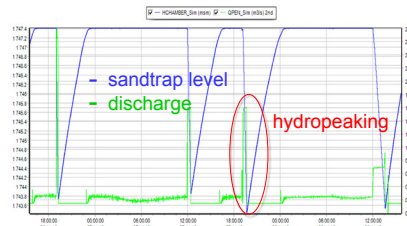
1. Commissioning follow-up

Comparison of the measured and simulated pressure at the penstock bottom during an emergency shutdown



2. Monitoring of the power plant during hydropeaking

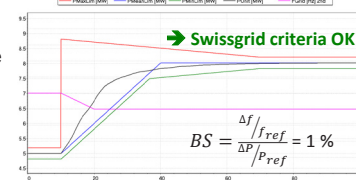
- Recording of the time evolution of the sandtrap water level and discharge during hydropeaking operating mode



3. Available power/energy assessment for ancillary services

Power setpoint, Permanent droop, Speed setpoint, Anti-Reset Windup, PID regulator

- Calibrated numerical model used to explore the behavior of the power plant
- assessment of the primary control potential



Contributors



Acknowledgments

This work is funded by SFOE, Swiss Federal Office of Energy (grant funding SI/501636-01), within the framework of the project «Demonstrator for flexible Small Hydropower Plant»

Schweizerische Eidgenossenschaft
Confédération suisse
Confederazione Svizzera
Confederaziun svizra
Office fédéral de l'énergie OFEN

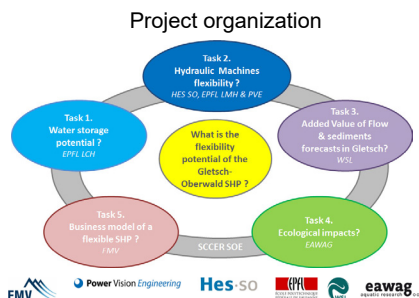
First insights on the production flexibility at the KWGO Power Plant

A. Gaspoz, V. Hasmatuchi, J. Decaix, C. Nicolet, M. Dreyer, J. Zordan, P. Manso, S. Crettenand, C. Münch-Alligné

Contact : HES-SO Valais, School of Engineering, Hydroelectricity Group, CH-1950 Sion, Switzerland, cecile.muench@hevs.ch

Context

The aim of the SMALLFLEX project is to investigate how small-hydropower plants (SHP) can provide **winter peak energy** and **ancillary services**, whilst remaining **eco-compatible**. The 15 MW Gletsch-Oberwald Power Plant, owned by FMV and commissioned at the end of 2017, has been selected as pilot site.



Source : Bulletin Electrosuisse, 02.2019, "Acceptation de l'énergie hydraulique alpine".

Available storage for the first campaign

For the first campaign of this project, the settling basin and the forebay tank, connected by two gates, have been used providing a storage volume of **3'700 m³**. This part of the identified storage allows to maintain a minimum available net head of 282 m required for a comfortable operation of the Pelton turbines.



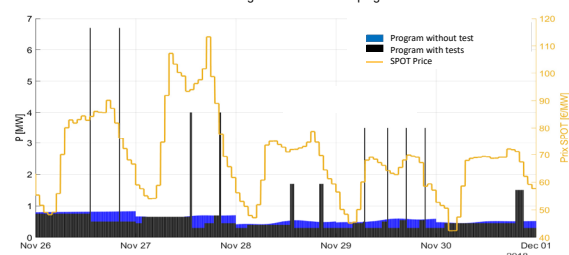
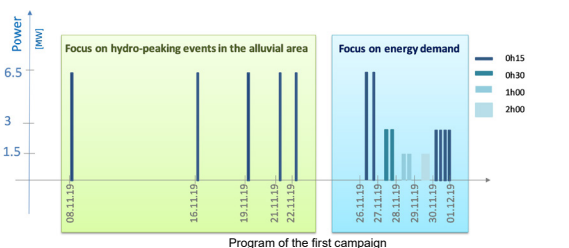
Settling Basin of KWGO



Forebay tank of KWGO

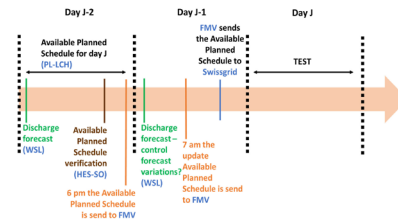
First campaign objectives & method

In November 2018, during three weeks, the competences of the research team have been gathered to explore experimentally the flexibility of KWGO. The first two weeks have been dedicated to induce 5 hydro-peaking events to monitor the impact in the downstream alluvial area. The last week was devoted to generate **several production peaks** taking into account the **energy demand** and the available storage.



Focus on the program of the 3rd week of the 1st campaign with/without the test & SPOT price.

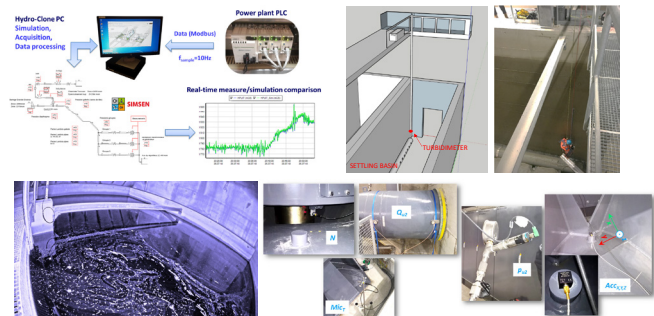
According to the discharge forecast and the available storage, a schedule for each day of test has been systematically prepared by the research team and sent to FMV.



Workflow for the 3rd week of test during the 1st SmallFLEX campaign

Monitoring in the power plant during the tests

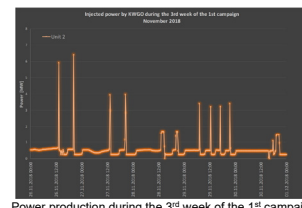
Since the acceptance tests of the turbines in July 2018, the HydroClone developed by PVE, partner of the project, is installed in the power plant. This monitoring system records all operating parameters of the power plant and provides access, from numerical simulation, to non-measured quantities. In parallel, a turbidimeter to monitor the sediments in the settling basin, a camera to supervise the free surface level in the forebay tank and several sensors on the turbine casing have been installed by HES-SO and EPFL PL-LCH.



Monitoring in the power plant : Hydroclone, turbidimeter, camera and several sensors.

Analysis

During the five days, the planned and effective productions show a minimum difference of around 1%. Through the use of the storage, the energy production has been increased of more than 40% for the five days considered¹.



Power production during the 3rd week of the 1st campaign

1. Zordan et al., Introducing flexibility in small hydropower plants, HYDRO 2019, Porto, Portugal

Conclusion and perspective

This first campaign demonstrated the possibility to use the settling basin and the forebay tank as a storage during periods of low discharge to maximize the energy production and the income adjusting the peak according to the SPOT price.

A second campaign is planned in 2020, doubling the available storage using part of the headrace tunnel of the power plant.

Acknowledgements

This project, developed in the framework of the SCCER-SoE, is financially supported by SFOE and FMV.

Contributors



HEATSTORE SWITZERLAND: New Opportunities for District Heating Network Sustainable Growth by High Temperature Aquifer Thermal Energy (HT-ATES) Storage

Guglielmetti L. *, Alt-Epping P. +, Birdsell D. ^^, De Oliveira Filho F. **, Diamond L. +, Driesner T. ++, Eruteya O. *, Hollmuller P. **, ^ Koumrouyan M., Makhloufi Y. *, Martin F. ; Meier P., Meyer M. ; Mindel J. ++, Moscariello A. *, Nawratil de Bono C. ; Quiquerez L. ; Saar M. ^^, Sohrabi R. ^, Spring, U. ; Valley B. ^, Van den Heuvel D. +, Wanner C. +.

Motivation

- Industry uses about 92% of their total energy requirement for generating process heat
- 50% of the total energy consumed in Switzerland is used to supply heat
- 86% of the required heat is generated by the burning of fossil fuel
- Households and services use about 92% of their total energy needs for heating applications
- Waste heat generated is continuously discharged into the environment



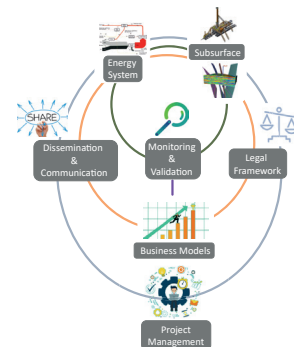
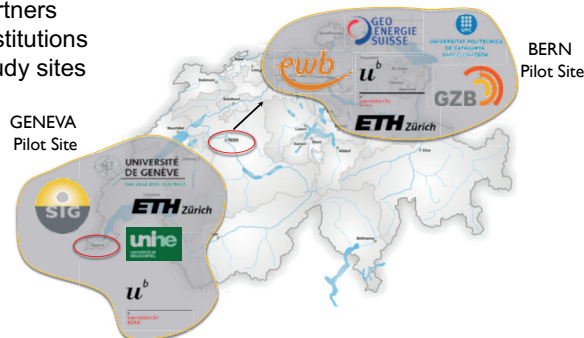
Let's convert waste heat into a resource

HEATSTORE

HEATSTORE aims at developing subsurface storage techniques to reduce wasting heat. A key technology is High Temperature (~25°C to ~90°C) Underground Thermal Energy Storage (HT-UTES). HEATSTORE is a European GEOTHERMICA ERA-NET co-funded project, with 24 contributing partners from 9 countries, composing a mix of scientific research institutes and private companies.

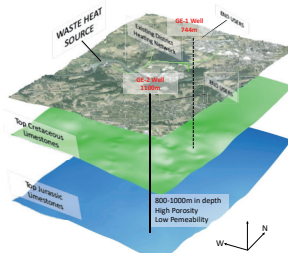
THE SWISS CONTRIBUTION

- 2 Industrial partners
- 4 Research institutions
- 2 HT-ATES study sites



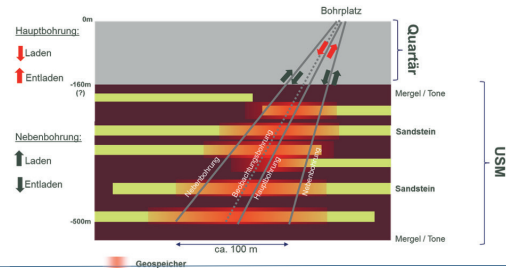
Geneva:

- Seasonal storage of waste heat from the Cheneviers incinerator
- Two potential reservoirs at depths between 500m and 1100m
- Heatstore contribution: subsurface characterization constrained by drilling and testing at two different locations (GEO-01 and GEO-02); Energy system integration modelling, which will be coupled to economical, regulatory, and social constraints, to potentially lead to a commercial implementation of the system in a following stage.



Bern:

- Seasonal storage of waste heat from the Bern-Forsthaus power plant.
- Three wells will be drilled to a depth of <500 m deep, into sandstone layers of the Lower Freshwater Molasse (USM)
- Assess the feasibility of an HT-ATES system and, if the results are encouraging, more wells will be drilled after the HEATSTORE project, to realize a fully functional heat storage system



*Department of Earth Sciences, University of Geneva. Rue des maraichers 13, 1205 Geneva (Switzerland) +University of Bern. Baltzerstrasse 3 3012 Bern (Switzerland)

**ETH Zürich - Geothermal Energy and Geofluids Group, Institute of Geophysics, Sonneggstrasse 5, 8092 Zürich (Switzerland)

***Department of F-A. Forel for environmental and aquatic sciences, University of Geneva. Bvd. Carl Vogt 66, 1205 Geneva (Switzerland)

++ETH Zürich - Institute of Geochemistry and Petrology, Clausiusstrasse 25, 8092 Zürich (Switzerland) *Energie Wasser Bern (EWB), Monbijoustrasse 11, 3001 Bern (Switzerland)

Services Industriels de Genève. Chemin du Château-Bloch 2, 1219 Le Lignon (Switzerland) ^University of Neuchâtel. Rue Emile Argand 11 2000, Neuchâtel (Switzerland)

luca.guglielmetti@unige.ch

AKNOWLEDGEMENTS

HEATSTORE (170153-4401) is one of nine projects under the GEOTHERMICA – ERA NET Cofund aimed at accelerating the uptake of geothermal energy in Europe. The project is subsidized through the ERANET cofund GEOTHERMICA (Project n. 731117) by the European Commission, RVO (the Netherlands), DETEC (Switzerland), FZJ-PJ (Germany), ADEME (France), EUDP (Denmark), Rannis (Iceland), VEA (Belgium), FRCT (Portugal), and MINECO (Spain). More information is available via <http://www.heatstore.eu>

Atténuation dans l'espace cours d'eau des éclusées résiduelles d'un bassin de démodulation: cas d'étude de Piotta



Marie Loverius, Pedro Manso, Giovanni De Cesare, Samuel Vorlet
 Platform of Hydraulic Constructions (PL-LCH), Ecole Polytechnique Fédérale de Lausanne (EPFL)



Introduction

L'aménagement hydroélectrique de Ritom se situe dans le canton du Tessin. Actuellement, l'aménagement turbine les eaux du lac de Ritom (CFF) et du bassin d'Airolo (AET) essentiellement pour l'approvisionnement électrique du réseau électrique CFF et AET. Dans le cadre du renouvellement de l'aménagement hydroélectrique de Ritom, la construction d'un bassin de démodulation d'un volume de 100'000 m³ est prévue à l'aval des centrales de Ritom (CFF) et de Stalvedro (AET) avec pour objectif l'atténuation des éclusées. Le projet comprend l'augmentation de la production à 60 MW impliquant un débit turbiné maximal de 29.3 m³/s.



Figure 1: Aménagement hydroélectrique de Ritom

De par la demande spécifique du réseau CFF, de fortes variations du débit turbiné infra-journalier sont à prévoir. Ces pics de production influenceront l'efficacité du bassin de démodulation et des éclusées résiduelles dans le Ticino sont à prévoir. Ce projet vise à étudier l'atténuation des éclusées résiduelles du bassin de démodulation dans l'espace cours d'eau.

Méthodes

Divers variantes ont été testées. La solution retenue consiste en la création d'une zone tampon sous forme de plaine alluviale par l'élargissement du cours d'eau aval. Cette zone tampon est délimitée du cours d'eau par une marche de 35 cm et a une rugosité plus élevée que le cours d'eau naturel.

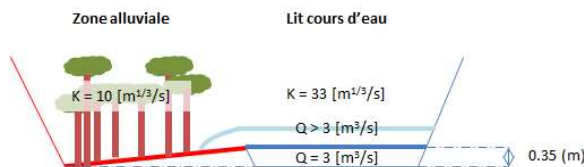


Figure 2: Plaine alluviale et cours d'eau naturel

Des simulations numériques sont réalisées à l'aide du logiciel Basement v.2.8 sur le tronçon aval du cours d'eau pour vérifier l'efficacité de la solution. Une modélisation 2D du tronçon est réalisée pour résoudre les équations de conservation de la masse et de la quantité de mouvement sur le domaine computationnel. Deux hydrogrammes de sortie du bassin de démodulation sont utilisés pour la modélisation hydraulique.

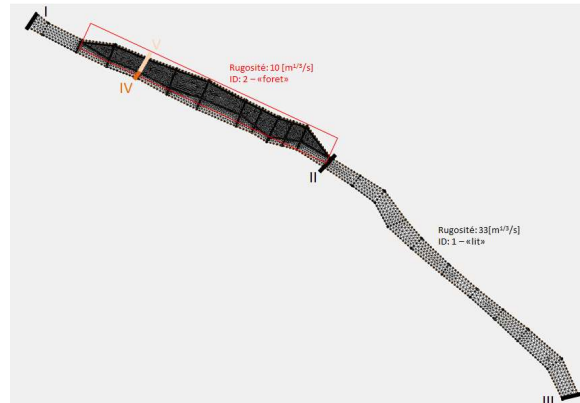


Figure 3: Domaine computationnel: cours d'eau naturel et élargissement

Résultats

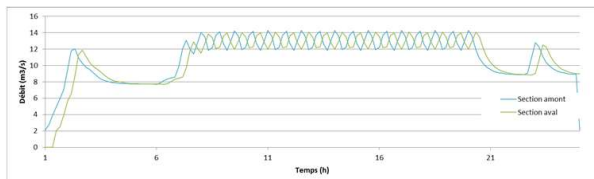


Figure 4: Evolution du débit en fonction du temps, hydrogramme de sortie du bassin de démodulation considérant des pics au débit maximum toutes les 30 min entre 6h et 19h, toutes les 3h entre 19h et 1h et pas de turbinage entre 1h et 6h; section amont (I) et section aval (III)

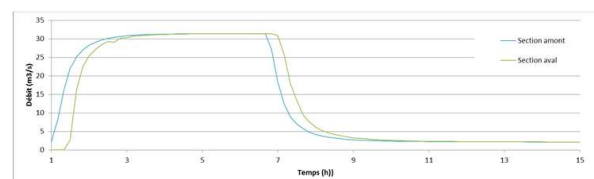


Figure 5: Evolution du débit en fonction du temps, hydrogramme de sortie du bassin de démodulation considérant un turbinage au débit maximum jusqu'au vidage complet du bassin (durée de 6h); section amont (I) et section aval (III)

Conclusion

Les résultats montrent que la solution proposée est relativement efficace pour les faibles débits (c.f. Figure 4). En effet, on observe une atténuation du débit de pointe à la zone aval ainsi qu'une atténuation des gradients pour les débits inférieurs à 15 m³/s. Pour les débits supérieurs (c.f. Figure 5), on n'observe aucune atténuation de l'hydrogramme. En effet, l'espace de stockage limité représente moins de 1% du volume à atténuer pour des débits importants. Une solution possible consisterait à activer l'espace de stockage avec une section critique contrôlée située à la fin de la plaine alluviale.

Références

- [1] Bieri, M., Zünd, B., Gasser, M., & Schleiss, A. (2016). 'Intervention strategies to mitigate hydropeaking: Two case studies from Switzerland. In HYDRO 2016 (No. EPFL-CONF-222964).
- [2] Hager, W. H., & Schleiss, A. J. (2009). *Constructions hydrauliques: écoulements stationnaires*. Lausanne : Presses polytechnique et universitaires romandes.
- [3] Pisaturo, G. R., Righetti, M., Dumbser, M., Noack, M., & Cavedon, V. (2017). The role of 3D-hydraulics in habitat modelling of hydropeaking events. *Science of The Total Environment*, 575, 219-230. doi: 10.1016/j.scitotenv.2016.10.046.
- [4] Schleiss, A. J. (2012). *Aménagements de cours d'eau*. Lausanne : Presses polytechnique et universitaires romandes.
- [5] Walter H. G. & Altinakar, M. S. (2011). *Hydraulique fluviale: écoulement et phénomène de transport dans les canaux à géométrie simple*. Lausanne : Presses polytechnique et universitaires romandes.

Directional-dependence of Mode I fracture toughness in Grimsel Granite

Morteza Nejati¹, Ali Aminzadeh^{2,3}, Martin Saar², Thomas Driesner³

¹ Department of Earth Sciences, ETH Zurich, Switzerland

² Geothermal Energy and Geofluids, Department of Earth Sciences, ETH Zurich, Switzerland

³ Institute of Geochemistry and Petrology, Department of Earth Sciences, ETH Zurich, Switzerland

Introduction

Many rock types behave anisotropic in their elastic and inelastic properties due to their complex micro-structure. Gischi et al. (2018) has recently demonstrated that rock anisotropy plays a critical role in the in-situ stimulation and circulation experiments in the deep underground laboratory at the Grimsel test site in Switzerland. It was concluded that the anisotropy of the mechanical properties such as elasticity, strength and fracture toughness must be taken into account to accurately predict the rock mass deformation and failure in those experiments (Dutler et al., 2018; Dambly et al., 2019). In this research, we present the experimental results on the directional-dependency of Mode I fracture toughness in Grimsel Granite.

Methodology

The stress intensity, or K-based approach, postulates that a crack extends when the stress, strain or a linear combination of the two, reaches a critical value in the region near the crack tip. Fracture growth criteria, such as maximum tangential stress and maximum tangential strain are based on the value of K_{Ic} to predict the crack growth under Mixed-Mode I/II conditions. The two energy-based fracture growth criteria, maximum energy release rate and minimum strain energy density, predict the onset of the crack growth using the critical values of the energy release rate (G_{Ic}) and the critical strain energy density (S_{Ic}). G_{Ic} and S_{Ic} are related to K_{Ic} through the elastic constants.

We point out that the measurement of K_{Ic} requires crack extension in a self-similar manner. While this typically happens in isotropic solids, it is likely that a Mode I crack in an anisotropic solid kinks towards the direction in which crack extension requires less fracture energy. This normally happens when K_{Ic} exhibits a strong directional dependency.

We recently modified the semi-circular bend (SCB) test to incorporate the elasticity anisotropy in the determination of the fracture toughness (Nejati et al., 2019a). The schematics of this test is shown in Figure 1a. This new test scheme allows to determine the fracture toughness at any orientation with respect to the principal directions (see Figure 1b).

In order to prepare the SCB samples, the original rock core, with the diameter of 120mm, was sub-cored in the direction normal to its axis in such a way that the foliation plane is parallel to the axis of the sub-core. A meter of the original core produced eight sub-cores with a diameter of 95 mm, each being cut to yield four SCB samples that have identical angles between the SCB base and the foliation. The SCB specimens from each sub-core were then notched with a thin cutting blade, so that all have the same angle, β , between the crack plane and the foliation. In total, a set of 29 samples with seven different angles, $\beta = 0^\circ; 15^\circ; 30^\circ; 45^\circ; 60^\circ; 75^\circ$ and 90° , were prepared. Once the peak load is measured for each experiment, the fracture toughness, K_{Ic} , is calculated using the geometry and material factors given in Nejati et al. (2019a). These values are then corrected if the fracture has not extended in a self-similar manner.

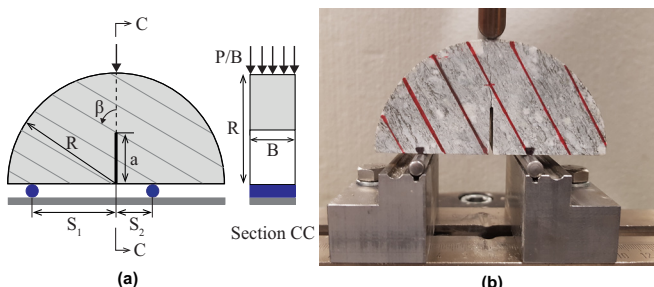


Figure 1. a) Schematics of the modified SCB test with asymmetric loading. b) Modified SCB test of Grimsel Granite with $S_1/R=0.6$.

Results and Discussion

Figure 2 illustrates the variations of the different measures of fracture toughness, K_{Ic} , G_{Ic} , and S_{Ic} , versus the angle β . The K_{Ic} data are obtained by correcting the apparent fracture toughness for the kink angle. The solid lines in K_{Ic} results represent the least-squares fit to the shown sinusoidal fit. It can be seen that the experimental data are fitted well using this sinusoidal variation. This gives supporting evidence for that yields a suitable type of variation of the critical SIF in an anisotropy plane. One can therefore use the two principal values of fracture toughness, measured along the two principal material directions, to determine the fracture toughness in any other direction.

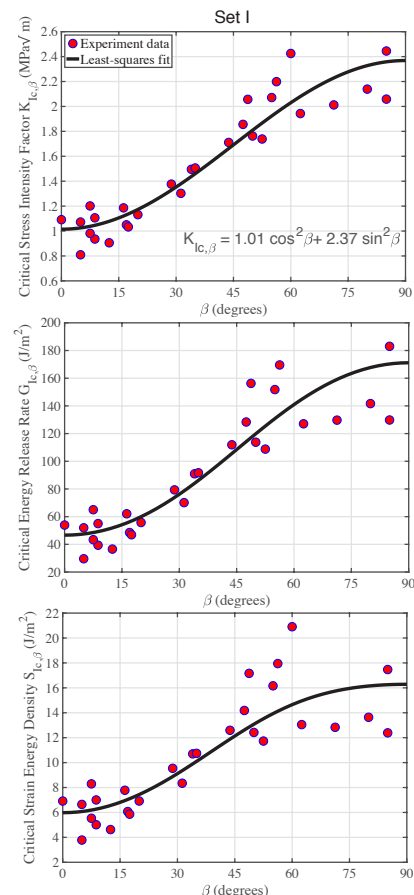


Figure 2. Variations of different measures of Mode I fracture toughness against β for a set of experiments on Grimsel Granite samples.

References

- Gischi, V., Doetsch, J., Maurer, H., et al., (2018). On the link between stress field and small-scale hydraulic fracture growth in anisotropic rock derived from micro-seismicity. *Solid Earth* 9 (1), 39–61.
 Dutler, N., Nejati, M., Valley, B., Amann, F., Molinari, G., (2018). On the link between fracture toughness, tensile strength, and fracture process zone in anisotropic rocks. *Engineering Fracture Mechanics* 201, 56–79.
 Dambly, M., Nejati, M., Vogler, D., Saar, M. O., (2019). On the direct measurement of the shear moduli in transversely isotropic rocks using the uniaxial compression test. *International Journal of Rock Mechanics and Mining Sciences* 113, 220–240.
 Nejati, M., Aminzadeh, A., Saar, M. O., Driesner, T. (2019a). Semi-circular bend test designed for mode I fracture toughness experiments in anisotropic rocks. *Engineering Fracture Mechanics* 213, 153–171.

Computational Modelling of Fine Sediment Release Using SEDMIX Device with Thrusters

Onate-Paladines, A. *, Amini, A., De Cesare, G.

Platform of Hydraulic Constructions (PL-LCH), EPFL. *Corresponding author: onateari8@aquacloud.net

EPFL



Introduction

- Problem:** Reservoir sedimentation occurs in dams worldwide, reducing the live storage available in the reservoirs.
- Possible solution:** Jenzer-Althaus (2011) tested a water stirring device (called SEDMIX) that keeps sediments in suspension, enhancing its release through the power intakes of the dam reporting a high efficiency.
- Background studies:** Numerical simulations for a prototype for the Trift reservoir have been carried out in the past by Amini et al. (2017) and Chraïbi et al. (2018), obtaining good results for sediment evacuation and determining the optimal location and dimensions of the device.
- Objective of the current work:** Numerically test the performance of SEDMIX at the Trift reservoir implementing thrusters instead of the previous configuration with water jets using ANSYS 2019 R1 software.

Methodology

- Compare the flow patterns in a regular tank obtained through numerical modelling (figure 1) with the experimental ones obtained by Jenzer-Althaus (2011).
- Considering various bottom clearances and a single phase flow, using the k-ε turbulence model and assuming a steady state flow.
- The jets were modelled as inner sources and the thrusters as a combination of inner sinks and sources to avoid refining elements.

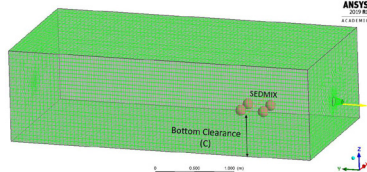


Figure 1: Numerical model of regular tank.

- Determine the sediment release at Trift reservoir and compare it with the one obtained with jets.

- The geometrical dimensions and location of the device were the optimal found by Chraïbi et al. (2018) (figure 2).
- A constant inflow Q_{in} of 21 m³/s, a relative pressure of 0 at the water intake and a multiphase flow were considered.
- It was assumed a concentration of 0.7 g/L of sediments, with a mean particle diameter (D_s) of 0.1 mm, and a density (ρ_s) of 2600 kg/m³.
- Three diameters of thrusters were considered. Each has its own thrust force (T) and rotational speed (n) that determined its maximum efflux velocity (U_0) as proposed by Albertson et al (1948) and its thrust coefficient (K_t) as suggested by Blaauw & Van de Kaa (1978):

$$U_0 \approx 1.60 \cdot n \cdot D \cdot \sqrt{K_t} \quad K_t = \frac{T}{\rho \cdot n^2 \cdot D^4}$$

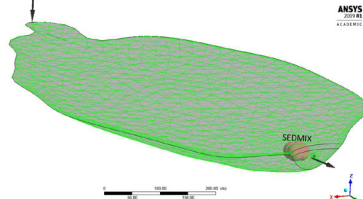


Figure 2: Numerical model of Trift reservoir

Results And Analysis

- The flow patterns obtained through numerical simulation of SEDMIX with water jets (figure 3a) are similar to the ones obtained by Jenzer-Althaus (2011) (figure 3b).
- With thrusters maintaining the same induced flow as the one considered for the jets, the flow velocity provided by them is too small to reproduce the flow patterns expected (figure 3c).
- Adjusting the thrusters to a higher velocity, a similar flow pattern was obtained (figure 3d).

References

- Jenzer-Althaus, J. Sediment evacuation from reservoirs through intakes by jet induced flow. PhD thesis, Ecole Polytechnique Fédérale de Lausanne; Switzerland, 2011.
- Amini, A.; Manso, P.; Venuleo, S.; Lindsay, N.; Leupli, C.; Schleiss, A. Computational hydraulic modelling of fine sediment stirring and evacuation through the power waterways at the Trift reservoir.; Hydro 2017, Seville, Spain.
- Chraïbi, A. Amini, A. Manso, P. Schleiss, A.J. Controlled fine sediment release through the power waterways by using a mixing device. SCCER-SoE Annual Conference. Switzerland, 2018.
- Albertson, M., Dai, Y., Jensen, R., & Rouse, H. Diffusion of submerged jets. ASCE Transactions, 1948. 648-697.
- Blaauw, H., & Van de Kaa, E. Erosion of bottom and sloping banks caused by the screwage of maneuvering ships, publication 202. Delft: Delft Hydraulics laboratory, 1978.

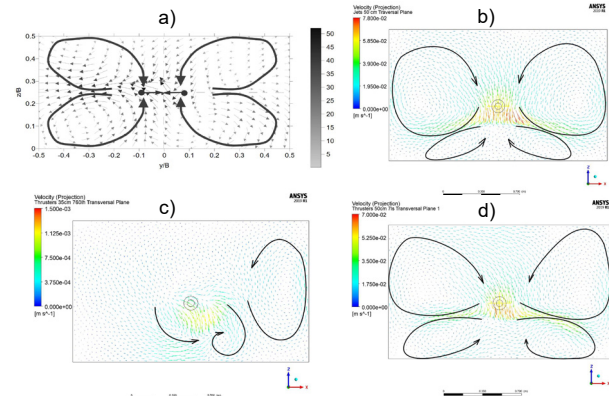


Figure 3: Flow patterns (transversal plane) obtained for a bottom clearance of 0.5 m: a) Experimentally (jets). b) Numerically (jets). c) Numerically (thrusters 760 l/h). d) Numerically (thrusters 7.2 l/s).

- The set of thrusters of 0.42 m were successfully calibrated to obtain the optimum sediment release (73 % of increment in evacuation), with a global induced flow of ~ 12.8 m³/s (3.2 m³/s per thruster) (figure 4). With this flow, the variation of the sediment velocity along the water column located at the vortex center resembles the one obtained for water jets, as shown in figure 5.

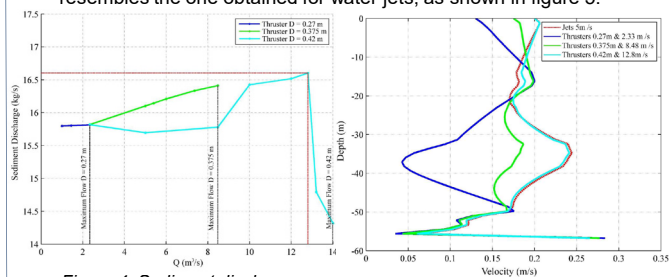


Figure 4: Sediment discharge with SEDMIX using thrusters of various diameters.

Figure 5: Variation of sediment velocity with depth for jets and thrusters.



Figure 6: SEDMIX to the 3D Dredger's™ floating platform

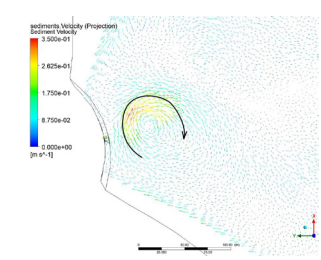


Figure 7: Rotational flow generated when using SEDMIX with thrusters.

Conclusion

- The numerical simulations showed similar patterns when using jets and thrusters, however, a higher induced flow is needed by the thrusters to be able to replicate the recirculation flow generated by the jets.
- For the Trift reservoir, the optimal thruster had a diameter of 0.42 m with an induced flow of 3.2 m³/s.
- Since the use of thrusters means no dealing with head losses, the power requirements could be less and the operational costs could be lower compared to the use of water jets.
- The experimental study of the device using thrusters is highly advised and the hydrodynamic behaviour in the reservoir should be further studied.

Assessment of a turbine model to predict cost effectively the far wake of a hydrokinetic farm

O. Pacot, D. Pettinaroli, J. Decaix, C. Münch-Alligné

Institute of Sustainable Energy, School of Engineering, HES-SO Valais-Wallis, Sion, Switzerland, olivier.pacot@hevs.ch

Context

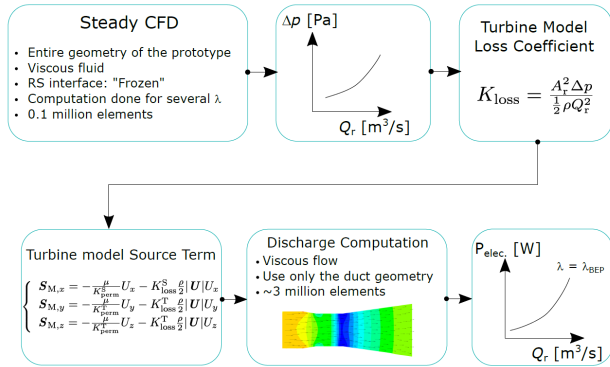
- To maximize the energy harvest from rivers, several hydrokinetic turbines [1,2] are assembled to form a farm, which requires to investigate the influence of the machines between each other and their influences on the local flow.
- To study these influences, numerical simulations are used. However, it requires to compute the free surface flow and all the interfaces between the stationary and rotating parts, which is time and computational expensive.

Objective

- To implement a simplified hydrokinetic model to save computational resources.

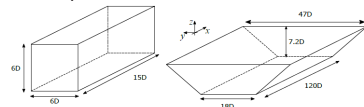
Hydrokinetic Turbine Model

The hydrokinetic turbine model (similar to the actuator disk) mimics the pressure drops experienced by the fluid from the runner [3]. The model requires a loss coefficient as parameter, which is obtained numerically using steady state simulations with a simplified computational domain.



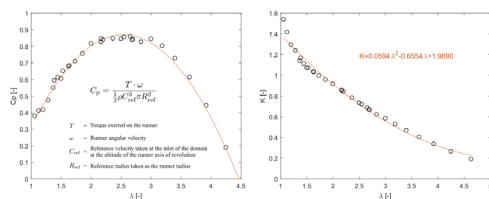
Numerical setup

Two different computational domains were designed using ANSYS ICEM CFD. The first one (**case 1**) uses a rectangular domain and was used to define the turbine model by steady and single phase simulations. The second one uses a trapezoidal domain and was used to simulate the flow field through a farm using once the full geometry of the machine (**case 2**) and once the turbine model (**case 3**). These simulations were unsteady and multiphase.



Computed performance and loss coefficient

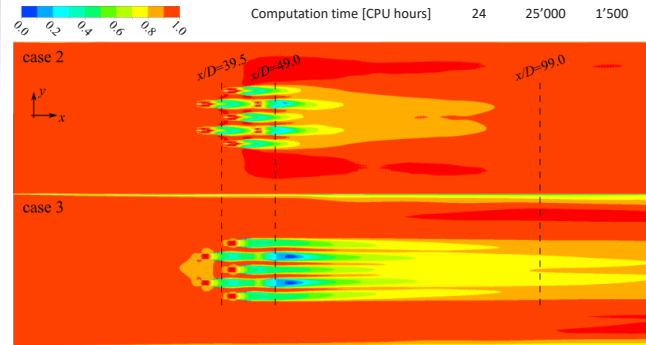
To establish the performance characteristic and the model parameter of the hydrokinetic turbine, several combination of the tip speed ratio λ were computed using ANSYS CFX R17.2. The Best Efficiency Point is reached for a $C_p=0.87$ [-] and a $\lambda=2.54$ [-]. Based on these simulations, the coefficient of resistance K can be computed and corresponds to 0.71 [-] at BEP [4].



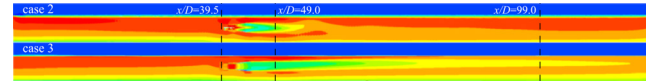
Results

- Case 3 required approximately 15 time less CPU hours and mesh resources compared to case 2.
- Case 2 shows a qualitative faster wake recovery, which might be attributed to the difference of mesh type and the lack of flow rotation in case 3.
- However, the quantitative comparison between case 2 and 3 shows that the difference in the horizontal velocity profile at $x/D=99.0$ is only of -13%.

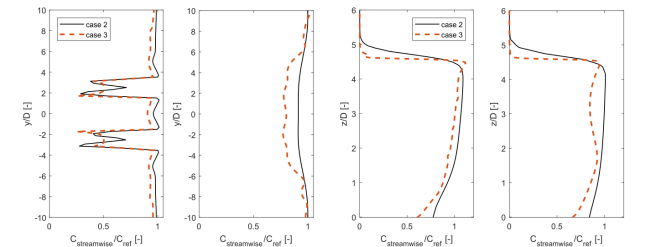
Case	1	2	3
Mesh size [Millions of elements]	0.1	45.6	2.9
Computation time [CPU hours]	24	25'000	1'500



Comparison of the instantaneous normalized streamwise velocity on the Oxy plane ($z/D=2.6$)



Comparison of the instantaneous normalized streamwise velocity on the Ozx plane ($y/D=0.0$)



Comparison of the instantaneous normalized velocity profiles. (a) horizontal profile at $z/D=2.6$. Left : $x/D=39.5$. Right: $x/D=99.0$. (b) vertical profile at $y/D=0.0$. Left : $x/D=39.5$. Right: $x/D=99.0$.

Conclusions

- A methodology was proposed to investigate faster the flow field passing through a hydrokinetic turbine farm.
- The comparison between the high resolution simulation (case 2) with the simplified one (case 3) showed acceptable discrepancies but a significant gain in mesh size and computation time.
- This methodology is well suited for an initial investigation on where to place hydrokinetic turbines in a river to get the maximum power output.

References

- [1] C. Münch, S. Richard, A. Gaspoz, V. Hasmatuchi, N. Brunner, "New Prototype of a Kinetic Turbine of Artificial Channels" Advances in Hydroinformatics, Springer, Singapore, 2018, pp. 981-996.
- [2] C. Münch, J. Schmid, S. Richard, A. Gaspoz, N. Brunner, V. Hasmatuchi, "Experimental Assessment of a New Kinetic Turbine Performance for Artificial Channels" Water 2018, Volume 10, Issue 3, 311.
- [3] Batten W M J, Harrison M E and Bahaj A S 2013 *Phil Trans R Soc A* 371 20120293-20120293
- [4] O. Pacot, D. Pettinaroli, J. Decaix and C. Münch, "Cost-effective CFD simulation to predict the performance of a hydrokinetic turbine farm". To be presented at the IAHWWG2019, 9-11 October 2019, Stuttgart, Germany.

LARGE-SCALE FIELD TESTS ON IMPULSE WAVES

Eva Sauter, Yuri Prohaska, Lukas Schmocker, Helge Fuchs, Robert Boes - VAW, ETHZ; Axel Volkwein - WSL

Motivation

Impulse waves, generated by avalanches, ice- or rockfalls, may seriously impair the reservoir of a hydropower plant. In some cases they even overtop or damage the dam and trigger hazardous flood waves (Fig. 1). Examining their potential impact is therefore an inevitable part of a comprehensive hazard assessment for hydropower reservoirs in alpine areas.



Fig 1: Impulse wave generation at Grindelwald Glacier Lake (Photo: Hans-Ruedi Burgener)

Field and laboratory tests

Within the CTI project FlexSTOR, both laboratory tests at VAW and prototype field tests at a gravel pit in Bülach were carried out to investigate the impulse wave generation and propagation. A test site was established in a 30 m deep gravel pit. The artificial reservoir was 15 m wide, 55 m long and had a still water depth of 1.5 m. A 40 m long steel ramp along the pit slope (37°) provided a sliding surface. The sliding mass was represented by a steel sledge (3 to 7 tons). The sledge could be released from different ramp positions to vary the impact velocity between 6 and 17 m/s. The resulting wave heights along the wave propagation path and the wave run-up were visually determined using gauge poles. A total of 13 tests were carried out in both field and model scale.

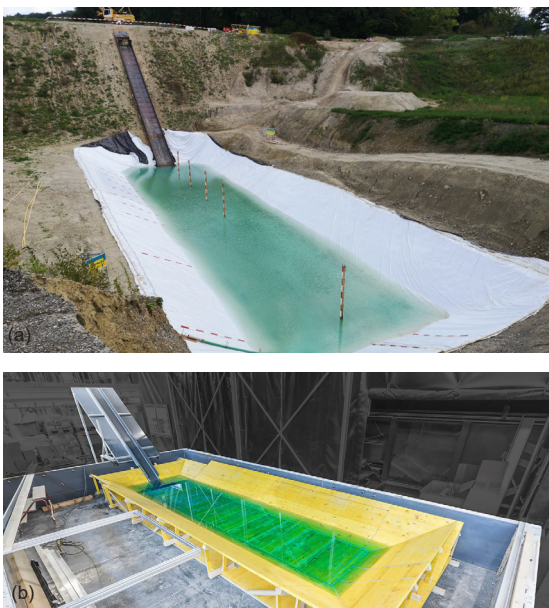


Fig 2: (a) Impulse wave field test site in gravel pit; (b) 1:10 scale model at VAW

Results

Due to the high sledge impact velocity in the field tests, a large splash is created, reaching up to 3/4 of the basin length. The maximum wave height occurs when a maximum of the sledge's energy has been transferred to the water body and the wave has propagated a certain distance from the impact location. The first and second waves are very steep and therefore start to break shortly after generation such that they finally propagate as long waves with reduced wave height.



Fig 3: Impact of sledge and splash generation in the field test

The maximum wave amplitudes were evaluated at the 5 gauges for all tests. Figure 4 compares the wave profiles measured for test V11 (maximum weight and impact velocity). Field and laboratory tests are in good agreement and the maximum wave amplitudes agree within $\pm 30\%$. Larger amplitudes show generally a better correlation, whereas smaller amplitudes may be partially affected by the measurement accuracy. The correlation however changes with the propagation distance as the amplitudes decrease. Overall, no significant scale effects have been determined and laboratory tests are consequently a feasible option to investigate slide induced impulse waves and the acquired results may be classified as robust and reliable.

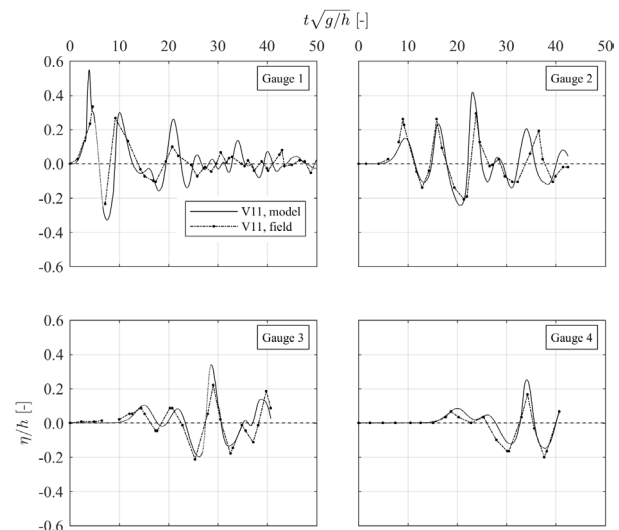


Fig 4: Comparison of relative wave amplitude at relative times measured in field (dotted line) and laboratory for tests (solid line)

Acknowledgement

This project is financially supported by Innosuisse with the industrial partner Kraftwerke Oberhasli (KWO). It is part of the FlexSTOR project and is embedded in the Swiss Competence Centre for Energy Research - Supply of Energy (SCCER-SoE) framework.

High Resolution Snow Melt and Runoff Modelling

Michael Schirmer, Massimiliano Zappa, Tobias Jonas

Motivation

The role of WSL and SLF within the SCCER-SoE is to develop and provide state-of-the-art snow cover and hydrological models suitable to predict inflow at the intake of hydropower plants as a basis for sediment management and for a flexible power production scheme. A high-resolution energy-balance-type snow model is applied enabling a realistic representation of small-scale processes in alpine terrain. Accounting for spatial variability is key to accurately assess changes in the distribution and frequency of runoff in small mountain catchments.

Methods

We used the state-of-the-art snowcover model JIM to describe the spatially variable water input at the soil surface. We recently refined the model to allow applications at very high spatial resolution by specifically accounting for small-scale processes relevant in mountainous environments. This model upgrade integrates developments such as a dynamically downscaling of radiation input delivered by Numerical Weather Prediction (NWP) models from 1 km to 250 m resolution and a subgrid-parameterization of snow covered fraction. Measured snow and air temperature data were assimilated in the model in order to initialize realistic start conditions for forecast values. Modelled surface water input was provided to the hydrological model PREVAH to simulate the intake to a hydropower plant. This model setup was applied to the demonstrator project “SmallFlex” (Task 5.1) in Gletsch, VS.

Results and Discussion

Shortwave radiation (SWR) was dynamically downscaled from coarser NWP models and include shading from the terrain.

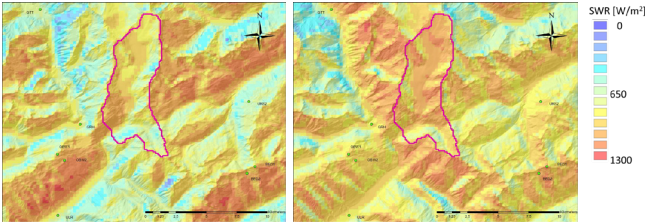


Figure 1: Modelled shortwave radiation for a clear day in June 2019 at 10 am (a) and 1 pm (b), respectively.

The resulting surface water input reacts on the spatial difference in shortwave radiation, but is also dependent on other factors as the current states of snow amount, snow covered fraction and snow wetness (next block) as well as other energy fluxes (Discussion).

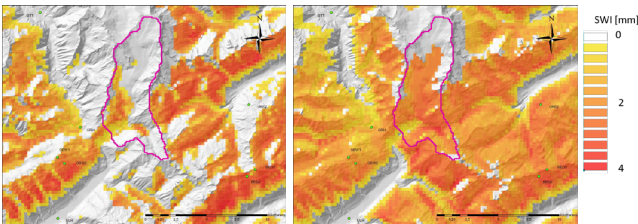


Figure 2: Modelled surface water input for one hour on a clear day in June 2019 starting at 10 am (a) and 1 pm (b), respectively.

Snow covered fraction (SCF) is dependent on modelled snow depth and terrain variables to account for snow depth variability. It is an important state variable since it strongly influences modelled surface water input (SWI). SWI is also dependent on the ability of snow to retain melt or rain water.

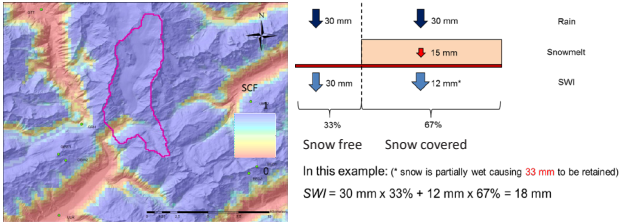


Figure 3: Modelled snow covered fraction for a day in June 2019 (a) and an example of the effect of SCF and snow retention capacity on surface water input (SWI) (b).

Surface water input (SWI) is provided to the hydrological model PREVAH, a high resolution semi-distributed model. This model chain is able to forecast the intake of the small hydropower plant of up to five days. A first analysis of the quality shows that the largest uncertainty is due to the input data. For example, the model receives too little precipitation at June 10. Ensemble of precipitation input may improve the forecast value significantly, especially for small alpine catchments where the localisation of high intensity precipitation is difficult to forecast correctly.

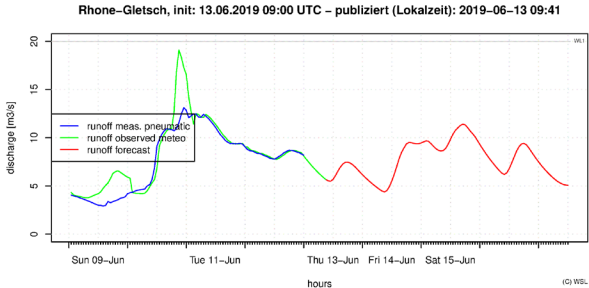


Figure 4: Intake of the small hydropower plant, in blue are observations, in green hindcast intake and in red forecast intake.

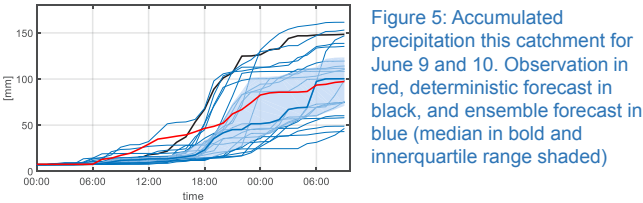


Figure 5: Accumulated precipitation this catchment for June 9 and 10. Observation in red, deterministic forecast in black, and ensemble forecast in blue (median in bold and innerquartile range shaded)

Discussion

Snow melt depends only indirectly on air temperature, while shortwave radiation is known to be the main driver for most situations. However, in most hydrological models snow melt is calibrated based on air temperature. This works fine for most situations, however, snow melt during rain-on-snow events can hardly be modelled correctly. Also for extreme situations, which are not well represented in the calibration data set, the less calibration-based energy balance model approach has a strong advantage. This is also true for future climate scenarios, for which the empirical relation between air temperature and runoff may change substantially.

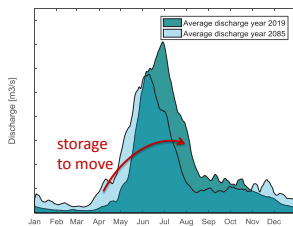
Multipurpose water reservoirs : a necessity for futur irrigation?

J. Schmid, J. Decaix, C. Münch-Alligné, A. Gillioz

HES-SO Valais, School of Engineering, Hydroelectricity Group, CH-1950 Sion, Switzerland, jeremy.schmid@hevs.ch

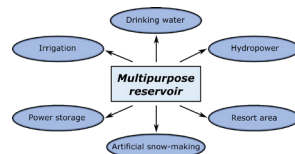
Context and Motivation

Switzerland, considered as the water tower of Europe, will not escape the problems related to water in the next years. Several causes indicate that such as fluctuating water supplies, local water shortages and also local geopolitical conflicts between the resources users.



Climate variations will change the hydrological regimes of alpine regions in the next years (2050-2100). The glaciers will slowly disappear inducing changes in the water regime by moving the peak earlier in the year [1]. So it is necessary to be able to store the water when we do not need to reuse it later in the year.

The challenges are the storage of winter water for the summer and that all users of the region are equitably supplied with water [2]. The multipurpose reservoir are part of the solution.



Multipurpose reservoirs:

- Significant contribution to having enough water available in the future
- Can compensate for the disappearance of glaciers
- Coordinate the multiple users of water
- Available for flood protection

Objective and Method

The project is divided into 4 distinct parts. The project aims to define the future hydrological regime of the region, to monitoring a part of the current network to make a numerical model that will allow to set up a master plan by the municipality of Val de Bagnes.

- Know the needs and future water resources in Val de Bagnes (VS)
- Develop a decision support for the management of water reservoirs
- Develop a general planning of the irrigation network

Modelling of current water yield and predicted future scenario



Monitoring of water supplies, water networks and water needs



Modelling of water networks, validation of models and future scenario simulations

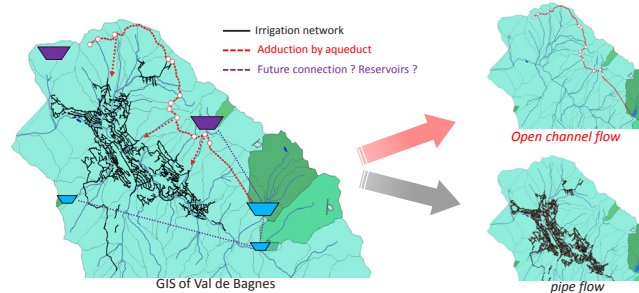


Network planning irrigation and tool to aid decision



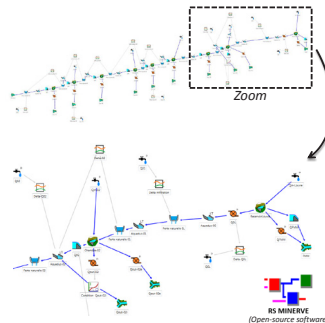
Water Network Modelling

- The numerical model is initially divided into two part. On the one hand the water adduction network (open channel flow (A)) and on the other hand the irrigation network distribution (pipe flow (B)).



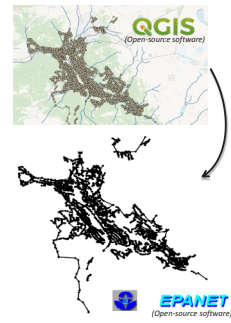
A) Macro level of the network

- Reservoirs modelling (H-V)
 - Lag-time river modelling
 - Level-discharge relation (spillway)
 - Time-series of flow discharge
 - Overall consumption of users
- Keywords : **flow - volume - level**



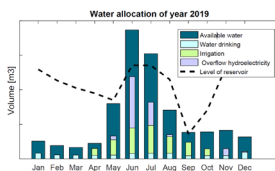
B) Specific level of the network

- Reservoir modelling (infinity volume)
 - Junction (with demand)
 - Pipe (head losses : Hazen-Williams)
 - Cane and valve (more than 2500)
 - Irrigation consumption
- Keywords : **pressure - flow**

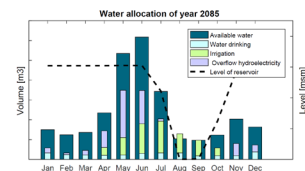


Perspectives and illustrative simulation

- Identify critical section of the network according to future scenario simulations
- Connecting the two numerical models
- Develop a holistic approach to water use in these watersheds
- Participate in the development of the master plan (connection - new reservoirs)



- Volume over the year is sufficient
- No drought condition in **average** year
- Spring period of filling the reservoir



- Volume over the year is sufficient
- More availability in winter (early)
- Drought condition in late summer

➤ New reservoir for storage in winter could reduce the drought period.

Acknowledgements



References

- [1] PNR 61. (2013). MontanAqua. Anticiper le stress hydrique dans les Alpes - Scénarios de gestion de l'eau dans la région de Crans-Montana-Sierre (Valais). Université de Berne.
- [2] Thut, W., Weingartner, R., & Schädler, B. (2016). Des réservoirs à buts multiples assurent l'alimentation en eau et en énergie. Université de Berne.
- [3] Manuela I. Brunner, hydrological simulation and products of Val de Bagnes (hydrological data)

Set-up and configuration of an ensemble Kalman filter for an operational flood forecasting system

Anne SCHWOB¹, Alain FOEHN¹, Javier FLUIXA², Giovanni DE CESARE¹

Contact: anne.schwob@epfl.ch

¹Laboratoire de Constructions Hydrauliques (LCH-EPFL), ²Centre de Recherche sur l'Environnement Alpin (CREALP)

INTRODUCTION:

To forecast riverine floods, short-range forecasts are normally provided. In such cases the initial hydrological conditions highly influence the predictability of a flood event.

The study evaluates the potential of an **ensemble Kalman filter (EnKF)** for the operational flood forecasting system in the Upper Rhone River basin (Fig 1). **Observed discharge data is used to update the initial conditions of the hydrological model.** Past flood events in the Reckingen subbasin (Fig. 1) are modelled to assess the robustness of the methodology and the quality of flood predictions.

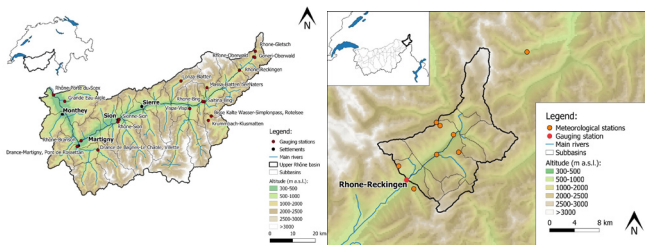


Figure 1: Maps of the Upper Rhone River basin (left) and the Reckingen subbasin (right) showing gauging stations and meteorological stations.

METHODOLOGY:

- Simulations are computed with the semi-distributed hydrological model RS MINERVE (Crealp, 2019).
- Three different discharge predictions are computed and compared:
 - Control simulation:** Open-loop scenario where discharge observations are not used to correct model initial conditions.
 - Volume based update (VBU) simulation:** Iterative approach correcting the initial soil saturation in order to generate the modelled water volume which has been observed over the 24 h before the forecast.
 - EnKF simulation:** Data assimilation (DA) method where the initial conditions of the model are updated based on the covariance matrices of the discharge observations and the model prediction (Fig. 2) (Evensen 1994).
- Forecast quality is evaluated based on the Kling-Gupta-efficiency (KGE) calculated for different lead times (Gupta et al., 2009):

$$KGE = 1 - \sqrt{(r-1)^2 + (a-1)^2 + (b-1)^2}$$

where r is the correlation coefficient, a is measure of variability and b is a measure of bias.

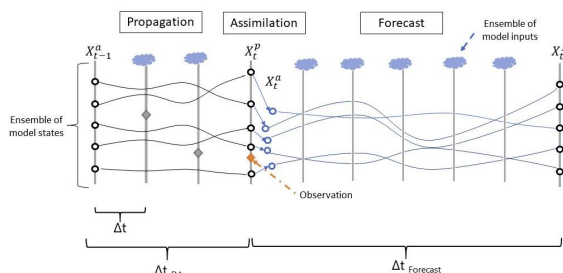


Figure 2: Schematic of the investigated EnKF where perturbed inputs are applied to an ensemble of model states (adapted Noh 2013).

RESULTS:

Figure 3 shows the streamflow prediction of the EnKF in comparison with the Control and VBU simulation as well as the observed discharge during an event in Reckingen in 2012. Figure 4 shows the KGE of the different simulation methods for four flood events in the Reckingen subbasin.

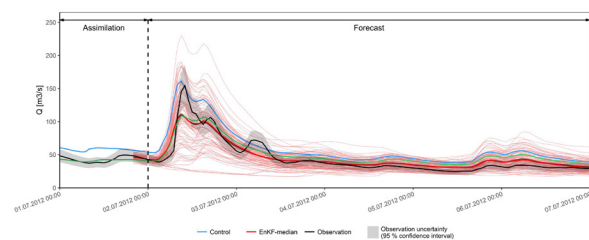


Figure 3: Example hydrograph during an event in Reckingen, July 2012.

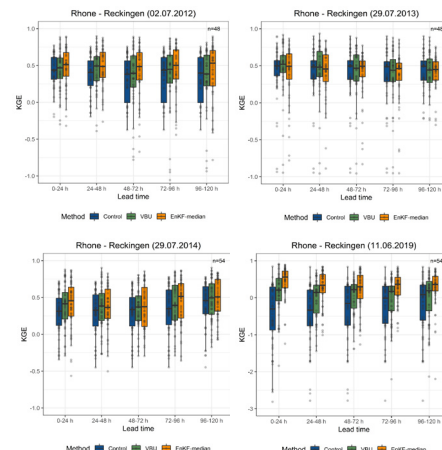


Figure 4: KGE of the three simulation methods for flood events in Reckingen in 2012, 2013, 2014 and 2019.

DISCUSSION AND CONCLUSION:

- For short lead times, the EnKF simulation outperforms the other two simulations. With an increased lead time the results depend on the event and the model calibration.
- To achieve good results with the EnKF, an appropriate model calibration and high-quality input data is needed.
- A DA method which specifically accounts for the time lag needed for streamflow routing could increase the robustness of the framework.

REFERENCES:

- Crealp, 2019. Available versions of RS MINERVE installers. URL <https://www.crealp.ch/download/install2/archives.html> (accessed 24.06.19).
- Evensen, G., 1994. Sequential data assimilation with a nonlinear quasi-geostrophic model using Monte Carlo methods to forecast error statistics. *Journal of Geophysical Research* 99, 10143.
- Gupta, H.V., Kling, H., Yilmaz, K.K., Martinez, G.F., 2009. Decomposition of the mean squared error and NSE performance criteria: implications for improving hydrological modelling. *Journal of Hydrology* 377, 80–91.
- Noh, S.J., Tachikawa, Y., Shiiba, M., Kim, S., 2013. Ensemble Kalman filtering and particle filtering in a lag-time window for short-term streamflow forecasting with a distributed hydrologic model. *J. Hydrol. Eng.* 18, 1684–1696.

GPR imaging of fractures in the Bedretto Lab

Alexis Shakas and Peter-Lasse Giertzuch

Motivation

The Bedretto Tunnel is located in Bedretto Valley (Ticino). Within the tunnel, at 2 km length (from a total of 5.2 km) there exists the Bedretto Underground Laboratory for Geosciences (BULG) - a research facility where the ETH Zurich and external partners are conducting experiments that focus on the safe and efficient extraction of geothermal heat from engineered geothermal systems within crystalline rock reservoirs.

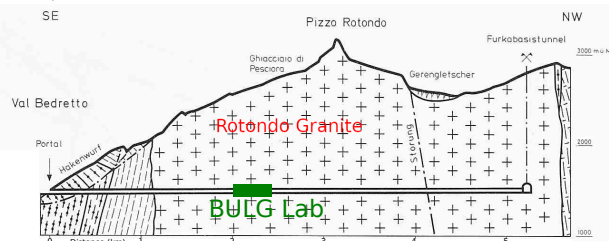


Figure 1. Geologic map of the Bedretto tunnel and the location of the BULG. This figure has been modified from Keller and Schneider (1982).

Fracture Detection using Ground Penetrating Radar (GPR)

Various geophysical techniques are used in the BULG to characterize the granitic rock mass and the presence of fractures along with their spatial properties. These properties, including the fracture density, aperture, length scale and orientation allow us to characterize processes such as fluid flow, heat dissipation and rock mechanical aspects such as hydraulic shearing and fracturing. One of the most promising methodologies for remote sensing of fractures (and associated processes) is ground penetrating radar; a technique that uses high-frequency (100 to 250 MHz) electromagnetic wave propagation and scattering.

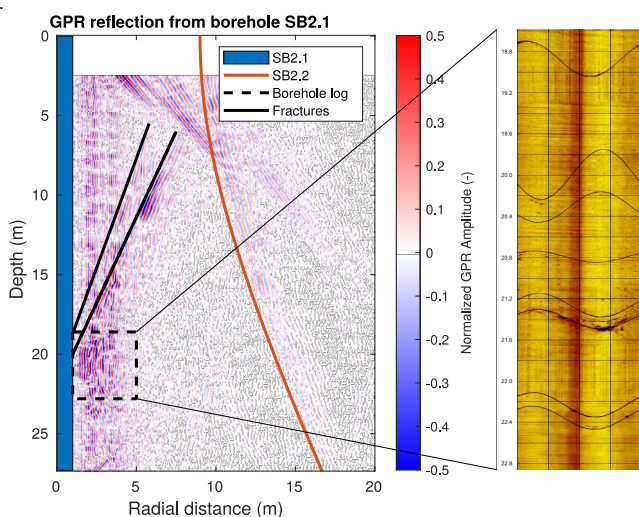


Figure 2. Left: Processed single-hole GPR reflection data from borehole SB2.1 (the borehole configuration is shown in the next figure). The first few meters are muted because strong reflections from the metal casing saturate the signal. The location of borehole SB2.2 is shown in red (computed from borehole trajectory alone). Two fractures are interpreted and shown in solid black lines. A region of the data where strong reflections arise is shown with a dashed rectangle. Right: The acoustic televiewer log reveals 8 fractures that intersect the borehole in the region identified by the GPR reflection image.

Forward Modeling of GPR reflections

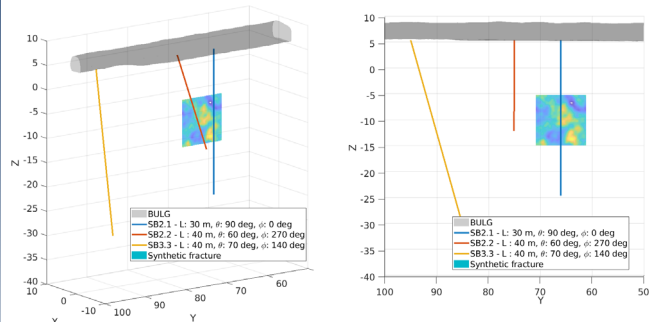
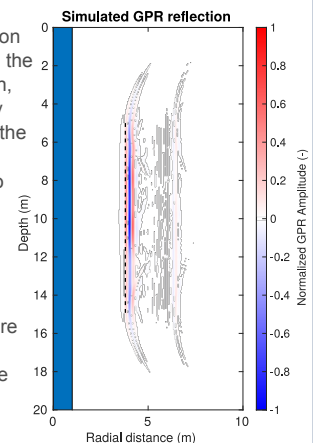


Figure 3. Top: Model showing the location and orientation of the three boreholes in the BULG. A synthetic fracture is also shown, of 10 m by 10 m extend and 4 m radially away from SB2.1. Color changes along the fracture plane correspond to aperture variations (blue to yellow corresponds to small to large apertures respectively - apertures vary in the sub-mm range).

Right: Simulated GPR reflection data corresponding to the fracture plane shown in the model above. The data were computed using the forward modeling scheme introduced by Shakas and Linde (2015). The dashed line reveals the real location of the fracture plane.



Discussion and Outlook

The Bedretto Underground Lab for Geosciences has been developing since 2017. Geophysical characterization of the granitic rock mass that surrounds the underground laboratory is of primary importance, prior, during and after any stimulation experiments, which can alter the natural state of the fracture network. Geophysical tools such as GPR offer a promising technology to delineate geometrical properties of fractures. This can be done in boreholes, as is presented here, but also along the tunnel wall.

Additionally, several geophysical imaging techniques can be combined in order to reduce the uncertainty in the measured properties by providing complementary information. For example, GPR uses electromagnetic waves to detect fracture aperture using the dielectric properties of the host rock and water (for water filled fractures). Additionally, active seismic methods will be used in a similar geometry to detect fracture aperture, while being sensitive to the density and elastic properties of the host rock and water. Such information can then be used in a joint modeling and inversion framework to constrain fracture permeability and assess permeability enhancement as a result of stimulation experiments.

Acknowledgements

The work presented here is part of the Bedretto project for Geo-energies (<http://www.bedrettolab.ethz.ch/>). The Bedretto team is to thank for all their individual contributions and effort in the project.

References

- Keller, F. & Schneider, T. R. (1982). *Geologie und Geotechnik*. Schweizer Ingenieur und Architekt, Heft 24.
- Shakas, A. & Linde, N. (2015). Effective modeling of GPR in fractured media using analytic solutions for propagation, thin-bed interaction and dipolar scattering. *Journal of Applied Geophysics*(116), 206-214

Tracing the CO₂ pathway in a faulted caprock: the Mont Terri Experiment of the ELEGANCY-ACT project

Alba Zappone, Melchior Grab, Anne C. Obermann, Claudio Madonna, Christophe Nussbaum, Antonio P. Rinaldi, Clément Roques, Quinn C. Wenning, Stefan Wiemer

1. Aims of the Experiment:

- Understanding how exposure to CO₂-rich water affects sealing integrity of faults in caprock (permeability changes; mechanical changes; induced seismicity);
- Imaging fluid migration along a fault and its interaction with the surrounding environment;
- Testing instrumentation and methods for monitoring fluid transport;
- Validate Thermo - Hydro - Mechanical - Chemical (THMC) simulations.

2. CS-D Experiment

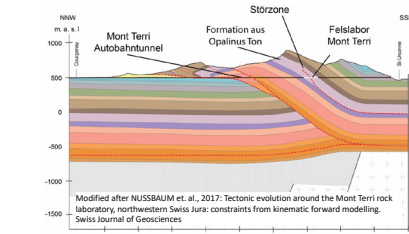


Fig 1: The Mont Terri laboratory, in NW Switzerland, is an international research underground facility for hydrogeological, geochemical geotechnical characterization of a clay formation (Opalinus Clay).

The CS-D experiment is located in a niche in the shaly facies of the clay. We inject CO₂-saturated water into the fault and monitor changes in pressure, pH and electrical conductivity in nearby wells. The portable mass spectrometer Miniruedi (cooperation with EAWAG) is used to monitor the chemical composition in the monitoring well. Seismic sensors in boreholes and along the walls of the niche will detect microseismicity, if any. Strain is measured through FO and SIMFIB (cooperation with LBNB).

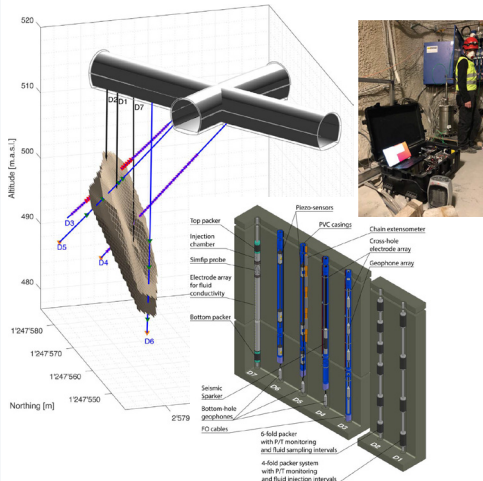


Fig 2: Layout of the experiment. The fault, c.a. 3 m thick, is at 12 to 30 m depth, and dips 60° towards SE. 7 boreholes are intersecting the fault and have been equipped with various instruments.

3. Injection tests

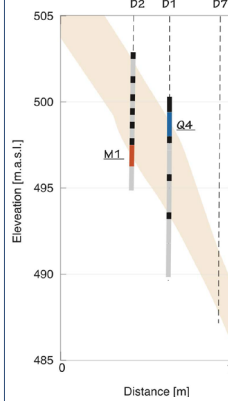


Fig 4: Injection borehole D1 (with interval Q4 highlighted) and monitoring well D2 (with interval M1 highlighted). Fault zone is shown in brown.

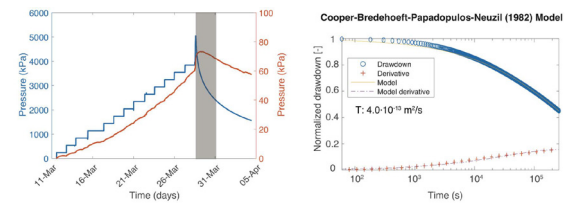


Fig 3: Right: Injection pressure in blue (injection into interval Q4) and observed fluid pressure in interval M1 (see Fig 4). Left: Analysis of constant head test with the Jacob and Lohman analytical solution provides an estimate of transmissivity in the order of 10^{-9} m²/s.

Several injection tests were performed to understand the system response to pressurization. The test shown in Fig. 3 is a prolonged step test in interval Q4. The pressure was increased by steps of 300 kPa, up to 4800 kPa. Each step was about 28-30 hours long. Analysis of pressure decay (3 days) with the Neuzil model provides an estimate of transmissivity in the order of 10^{-13} m²/s ($\sim 10^{-21}$ m² permeability).

4. Geophysical monitoring

The experiment is monitored using active and passive seismic methods. Two sets of sensors consisting of piezoelectric transducers and grouted geophones were installed for this purpose (Fig. 2). During the pumping tests, no induced seismicity was detected. Further analysis of data, including also recordings during gallery excavation activities (Fig. 5), is ongoing.

Active seismic measurements have been performed with hammer sources in the gallery and a P- and S-wave sparker sources in the boreholes. During the injection test and the long-term injection, these measurements are repeated.

In Fig 6, an example trace is shown, which has been recorded during injection tests. Variations in arrival times were detected which are larger than the variability within repeated shots (Fig 6. left). The data is currently processed for tomographic travel time imaging.

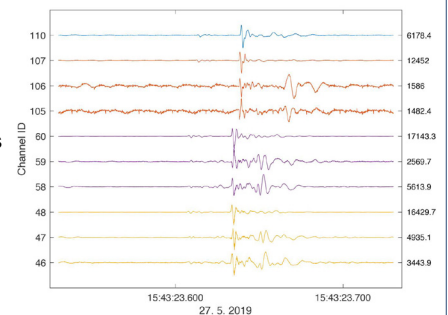


Fig 5: Microseismic event recorded with geophones during drilling activities in the laboratory. Traces of the same color are recorded with different components of the same geophone.

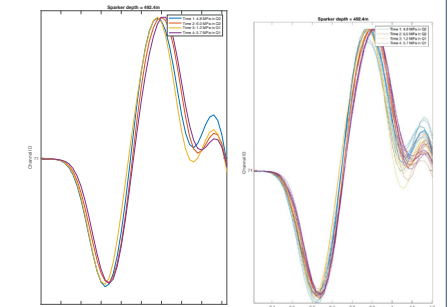


Fig 6: Example trace from time-lapse active seismic monitoring during injection tests after (right) and before (left) stacking.

5. Start of the long term injection of CO₂ saturated water

Mid June 2019, the long-term injection of CO₂ saturated water was started, together with repeated active seismic and ERT measurements. Since then, the injection takes place under constant pressures of 4500 kPa. The injection rates are small (< 0.1 ml/min) and up to now slightly decreasing with time.

Acknowledgements: We thank Christoph Bärlocher, David Jaeggi, Edgar Manukyan, Hansruedi Maurer, Linus Villiger, Marija Lukovic, Nils Knornschild, Nima Gholizadeh, Paul Bossart, Semih Demir, Senecio Schefer, Thierry Theurillat, and Thomas Mörgeli for technical support, scientific advice, and/or on-site assistance. ACT ELEGANCY, Project No 271498, has received funding from DETEC (CH), FZJ/PtJ (DE), RVO (NL), Gassnova (NO), BEIS (UK), Gassco AS and Statoil Petroleum AS, and is cofunded by the European Commission under the Horizon 2020 programme, ACT Grant Agreement No 691712.